

THE UNIVERSITY OF MICHIGAN
COLLEGE OF ENGINEERING
Department of Mechanical Engineering

Final Report

A STUDY OF HIGH-SPEED MILLING

Part II. The High-Speed Milling of Titanium Alloys

L. V. Colwell
L. J. Quackenbush

ORA Project 05038

SP-472

under contract with:

J. E. RAMSEY
LA CANADA, CALIFORNIA

administered through:

OFFICE OF RESEARCH ADMINISTRATION

ANN ARBOR

December 1962

en gn

UMR4683

TABLE OF CONTENTS

| | Page |
|---|------|
| LIST OF TABLES | v |
| LIST OF FIGURES | vii |
| ABSTRACT | xi |
| INTRODUCTION | 1 |
| I. QUALITATIVE SUMMARY AND INTERPRETATION OF RESULTS | 3 |
| A. Unique Process Characteristics | 3 |
| B. Potential Applications | 4 |
| 1. Tape-controlled milling machines | 4 |
| 2. High-feed-rate mills | 5 |
| 3. Superimposed ultrasonics | 5 |
| 4. Substitute processes for grinding | 5 |
| C. Recommended Next Steps in the Development | 6 |
| II. DETAILED LABORATORY RESULTS | 7 |
| A. Tool-Wear Studies | 7 |
| 1. Air turbine tests | 8 |
| 2. Single-point-tool tests | 9 |
| B. Cutting-Temperature Studies | 11 |
| 1. Tests with imbedded thermocouple | 11 |
| 2. Tests with lead sulfide cell | 12 |
| C. Studies of Forces, Standing Waves, and Chip Segmentation | 12 |
| APPENDIX A. TEMPERATURE MEASUREMENTS | 37 |
| I. Lead-Sulfide, Infrared Detector | 38 |
| A. Physical configuration | 38 |
| B. Performance characteristics | 38 |
| C. Temperature vs. output voltage calibration | 39 |
| D. Bridge circuitry | 40 |
| E. Effects of time constant on results | 41 |
| F. Location of cell relative to workpiece | 42 |
| G. Oscilloscope triggering | 42 |
| II. Thermocouple Imbedded in Tool | 43 |
| APPENDIX B. STRAIN-GAGE INSTRUMENTATION | 45 |

TABLE OF CONTENTS (Concluded)

| | Page |
|--|------|
| APPENDIX C. CUTTING-FORCE MEASUREMENTS | 49 |
| APPENDIX D. WEAR STUDIES | 51 |
| I. Single-Tooth Cutter | 52 |
| II. Multitooth Cutters | 53 |
| III. Observations on Cutter Wear | 54 |

LIST OF TABLES

| Table | Page |
|---|------|
| I. Wear Tests on Air Turbine with a Range of Cutter Diameters | 7 |
| II. Single-Tooth Cutter Wear: Variable Speed | 10 |
| III. Single-Tooth Cutter Wear: Variable Feed Rate | 10 |
| B-I. Semi-Conductor Strain-Gage Data | 47 |
| D-I. Typical Data Sheet (Three Different Single-Tooth Wear Tests) | 56 |
| D-II. Relation of Various Parameters for Multitooth-Cutter Wear Studies | 57 |
| D-III. Typical Data Sheet (Test Runs Nos. 1, 2, and 3) | 58 |
| D-IV. Typical Data Sheet (Test Runs Nos. 4 and 5) | 59 |

LIST OF FIGURES

| Figure | Page |
|---|------|
| 1. Tool wear vs. feed rate (A-110 titanium). | 14 |
| 2. Tool wear vs. volume of metal cut (B-120 titanium). | 15 |
| 3. Tool wear vs. volume of metal cut (A-110 and C-120 titanium). | 16 |
| 4. Tool wear vs. volume of metal cut (A-110 titanium). | 17 |
| 5. Wear vs. volume removed (A-110 titanium). | 18 |
| 6. Tool temperature at imbedded thermocouple (3000 fpm). | 19 |
| 7. Tool temperature at imbedded thermocouple (1500 fpm). | 20 |
| 8. Tool temperature at imbedded thermocouple (A-110 titanium). | 21 |
| 9. Tool temperature at imbedded thermocouple (C-1018 steel). | 22 |
| 10. Tool temperature at imbedded thermocouple (original chart records). | 23 |
| 11. Tool temperature at imbedded thermocouple (records for C-1018 steel). | 24 |
| 12. Tool temperature at imbedded thermocouple (records for A-110 titanium). | 25 |
| 13. Tool-flank temperature vs. cutting speed for five different metals. | 26 |
| 14. Tool-flank temperature vs. cut thickness for five different metals. | 27 |
| 15. Tool-flank temperature vs. cutting time (A-110 titanium). | 28 |
| 16. Tool-flank temperature vs. cutting time (C-120 titanium). | 29 |
| 17. Tool-flank temperature vs. cutting time (B-120 titanium). | 30 |
| 18. Tool-flank temperature vs. cutting time (C-1018 steel). | 31 |

LIST OF FIGURES (Continued)

| Figure | Page |
|---|------|
| 19. Tool-flank temperature vs. cutting time (Armco iron). | 32 |
| 20. Comparison of three grades of titanium as replotted from Figs. 15, 16, and 17. | 33 |
| 21. Oscilloscope records of internal vibrations of titanium A-110 test specimen. | 34 |
| 22. Oscilloscope records for tangential cutting force and internal vibrations of brass test specimen. | 35 |
| 23. Oscilloscope records illustrating behavior characteristics of aluminum and brass test specimens. | 36 |
| A-1. Temperature measuring set-up used to obtain data plotted in Figs. 13-20. | 63 |
| A-2. Oscilloscope trace for one of lead-sulfide cells tested. | 64 |
| A-3. Bridge circuit used with lead-sulfide cell for temperature measurement. | 64 |
| A-4. Oscilloscope trace of tool-flank temperature (A-110 titanium, 1-in. cut). | 65 |
| A-5. Oscilloscope trace of tool-flank temperature (A-110 titanium, 1/4-in. cut). | 65 |
| A-6. Temperature-measuring set-up used to obtain data plotted in Figs. 6-12. | 66 |
| B-1. Ballast circuit used with strain gages. | 67 |
| B-2. Location of strain gages used to monitor-internal vibrations as displayed in Figs. 21 and 22. | 67 |
| C-1. Set-up used to obtain cutting-force records shown in Figs. 22 and 23. | 68 |
| D-1. Set-up for studies of single-tooth-cutter wear. | 69 |
| D-2. Relation between chip thickness and feed rate. | 70 |

LIST OF FIGURES (Concluded)

| Figure | Page |
|--|------|
| D-3. End view of partially enclosed set-up showing instrumentation. | 71 |
| D-4. Open end view of cutter and workpiece orientation. | 71 |
| D-5. Common flank wear profile. | 72 |
| D-6. Sketch of typical wear of 4-fluted tungsten carbide milling cutter. | 72 |

LIST OF FIGURES (Concluded)

| Figure | Page |
|--|------|
| D-3. End view of partially enclosed set-up showing instrumentation. | 71 |
| D-4. Open end view of cutter and workpiece orientation. | 71 |
| D-5. Common flank wear profile. | 72 |
| D-6. Sketch of typical wear of 4-fluted tungsten carbide milling cutter. | 72 |

ABSTRACT

Feed rates in excess of 1000 ipm have been attained successfully in milling titanium alloys with solid carbide end mills. Spindle speeds approaching 20,000 rpm have made it possible to reduce the time of individual tooth contacts to about 200 μ sec. At these conditions it has been demonstrated that tool wear is orderly and predictable and not disproportionately high in relation to the very high rates of metal removal.

Results reported from this investigation show that temperature can be reduced by increasing the size of cut beyond a minimum determined by system rigidity. It is demonstrated also that high-frequency vibrations combine with short cutting times to greatly attenuate the natural trend toward higher temperatures and tool wear with increases in cutting speed and size of cut.

INTRODUCTION

This report is divided into three major sections. Section I presents a summary and qualitative interpretation of the results of this particular investigation. Section II presents a detailed summary of the actual test data and their correlation. The third section, which comprises Appendices A, B, C, and D, presents the details of set-up, calibration and test procedure for each of the laboratory investigations.

This second investigation was devoted to a further study of the feasibility of developing substantially higher rates of metal removal in the high-speed milling of titanium. The ultimate objective was to increase the rate of metal removal in cubic inches per minute or in square inches of machined surface per minute. This is directly related to the feed rate in inches per minute (ipm), which can be increased substantially only by resorting to higher cutting speeds and spindle speeds.

The first investigation¹ demonstrated the feasibility of attaining very high feed rates in this manner. It also yielded some unique information which was studied in greater detail in this second investigation. Among the points brought out in the first investigation were:

- (a) That metals can be cut at high cutting speeds providing the cutting time is limited to the order of 0.001 sec; that is, contact time between the cutter and the workpiece appeared to be limited to about 1 msec.
- (b) It was also indicated that a cut can be too thin. Among the observations supporting this conclusion were the following: the chips seemed to be hotter when the theoretical chip thickness was relatively thin, and abnormally high tool wear seemed to be associated with this condition.
- (c) Even though the actual feed rate in the first study did not go much beyond 200 ipm, projections from these results demonstrated the feasibility of very high feed rates, perhaps approaching 1000 ipm.
- (d) The use of micro-mills with fine teeth appeared to be a logical approach to accomplishing the high feed rates.

The current project was set up to develop better quantitative information on the necessary cutting conditions with regard to cutting speed, size of cut, feed rates, and limiting time of individual tooth contact with the work material in forming a single chip. A program was set up to develop this informa-

tion through measurements of forces and power, tool temperatures, and rate of tool wear.

I. QUALITATIVE SUMMARY AND INTERPRETATION OF RESULTS

The results obtained in this investigation have been positive in that they have (1) reconfirmed the feasibility of achieving very high feed rates through the use of high cutting speeds in milling titanium, and (2) indicated the existence of a workable latitude of cutting conditions.

The first program predicted feed rates up to 1000 ipm compared with commercial rates seldom exceeding 25 ipm. It was expected that special fine-toothed micro-mills would have to be used to achieve this result. In the current program, feed rates as high as 1200 ipm were accomplished successfully and without the use of micro-mills. Instead, standard commercial 4-tooth end mills proved very satisfactory for feed rates in the range between 240 and 1000 ipm. It is expected that this range can be extended further in both directions by increasing rigidity beyond that of the laboratory set-up.

A. UNIQUE PROCESS CHARACTERISTICS

The applications and limitations of the process are determined by three important and unique factors:

- (1) Most important is the time of contact between the cutter and workpiece in forming a single chip. This time must be of the order of 3 msec or less for metals like steel or titanium. It may be substantially longer for aluminum, brass, magnesium, copper, and similar materials. This requires balancing the combination of cutting speeds, cutter diameter, and the thickness of the layer of metal to be removed from the workpiece. Thus contact time limits the useful range of cutting conditions for titanium to the following:
 - (a) Spindle speed: 10,000 to 25,000 rpm
 - (b) Cutter diameter: up to 1 in.
 - (c) Thickness of metal removed per pass: up to 0.050 in.
- (2) High cutting speed is useful only so far as it:
 - (a) Reduces the tooth-contact time
 - (b) Sustains high-frequency chip segmentation, which in turn reduces temperature as a result of reduced energy requirements

Otherwise, increasing the cutting speed generally results in higher temperature, which increases the rate of tool wear.

Shorter tooth-contact time and chip segmentation operate only to inhibit or hold back this general trend. In other words, higher cutting speeds should be resorted to only when one or more of these factors proves to be effective in reducing tool wear.

- (3) System rigidity plays a very important role in the process since it determines both the maximum and the minimum chip thicknesses which can be machined satisfactorily. The minimum is determined by abnormal temperature conditions arising out of increasing dominance of frictional rubbing with thin cuts. Therefore, unless a certain minimum of system rigidity is achieved, the gap between maximum and minimum chip thickness may be closed up completely, thereby preventing any machining at high speeds. Obviously, spindle rigidity becomes a major problem at speeds in the range 10,000 to 25,000 rpm.

B. POTENTIAL APPLICATIONS

At least four potential applications suggest themselves from the results of the current program.

- (1) The first of these is in adaptation to existing multi-axis, tape-controlled milling machines.
- (2) The second involves the development of new milling machines with feed-rate capability beyond that of any machine now in existence.
- (3) The third concerns the adaptation of ultrasonic vibrations to milling cutters operating at low cutting speeds in order to obtain the benefits of high-frequency chip segmentation which occurs naturally at the high cutting speeds used in this study.
- (4) A fourth possible application would be the development of substitute processes for grinding, especially for the lower-strength materials like aluminum and magnesium.

1. Tape-Controlled Milling Machines

The results of this study demonstrate the feasibility of using a single-tooth milling cutter in a high-speed spindle which could be adapted to existing tape-control machines. This combination would make it possible to machine high-strength materials such as titanium on tape-controlled machines at the

limit of their feed-rate capability. This requires only the development of a sufficiently rigid, high-speed spindle and the development of rapid cutter regrinding practices in order to make the application both practical and economical.

2. High-Feed-Rate Mills

The full feed-rate potential of the high-speed milling process can be achieved only through the use of cutters with more than one tooth, numbering perhaps as many as 8 to 10 teeth as large as 1 in. in diameter. With such cutters a spindle operating at a speed in the range of 10,000 to 12,000 rpm would permit the use of feed rates ranging from 100 ipm up to 1000 or more ipm. To become practical and economical, this application, like the application to tape-controlled mills, requires the development of a rigid, high-speed spindle and a new process of tool resharpening. It would also require the design and development of new milling machines capable of the higher ranges of feed rates made possible by this process.

3. Superimposed Ultrasonics

As reported in Part I of this Final Report, the study of shock waves and internal vibrations in workpieces demonstrated that the energy required to remove a unit volume of metal is considerably reduced in the presence of such vibrations. This in turn reduces the temperatures which are accompanied by the lower rates of tool wear. Such vibrations occur naturally and with sufficient intensity at high cutting speeds. However, they do not occur with sufficient intensity at low cutting speeds except with such materials as magnesium and leaded brass. Therefore the reduced energy consumption and, more particularly, the lower temperatures can be achieved only through artificial generation of high-frequency vibrations. A probable further benefit of such an application would be better control if not elimination of the problem of chatter. Ultrasonic frequencies would be high enough for this purpose only at the lower spindle speeds which are in common use today. Some success with this type of application has already been reported in Russian technical literature.

4. Substitute Processes for Grinding

Experience obtained in this program demonstrates the feasibility of cutting materials like aluminum, brass, magnesium, and copper at cutting speeds up to 15,000 to 16,000 fpm or approximately three times the speed normally used for grinding. Thus it is feasible to substitute a milling cutter for a grinding wheel and thereby to improve the production rate and the finished product with the materials, which as a rule are relatively difficult to grind satisfactorily.

C. RECOMMENDED NEXT STEPS IN THE DEVELOPMENT

(1) The most important development necessary for successful shop utilization of high-speed milling is an exceptionally rigid, high-speed spindle capable of operating at speeds of 10,000 to 12,000 rpm, and delivering 20 to 50 hp. It would appear that the necessary rigidity is most feasible in a spindle-with externally pressurized, hydrostatic bearings.

(2) Electrochemical methods would appear to qualify for the purpose of accomplishing adequate, low-cost tool sharpening. However, this process also requires some development.

(3) The application of ultrasonics to milling at present commercial speeds needs to be investigated further before equipment for this type of application can be designed properly. It is recommended that a study be made wherein ultrasonic vibrations are first superimposed on the workpiece so as to demonstrate whether the desired benefits can actually be achieved. If it is demonstrated that they can be achieved, the second step could be devoted to developing techniques for vibrating the cutting tool itself.

(4) The possibilities for developing substitutes for grinding could be investigated by the substitution of a suitable milling cutter for the grinding wheel in a surface grinding operation. Among the immediate objectives in such an investigation would be to determine the practical limits of chip thickness and table or feed traverse rates in relation to the surface finish and size control which one must achieve in any process that is to be substituted for grinding.

II. DETAILED LABORATORY RESULTS

The laboratory investigations carried out in this study consisted of three major studies: (1) of tool wear, (2) of cutting temperatures, and (3) of forces, standing waves, and related chip segmentation. The phenomenon of standing waves and its relationship to segmentation, was dealt with in Part I of this Final Report,¹ but some additional work has been done since that time and is presented below.

A. TOOL-WEAR STUDIES

The tool-wear studies were performed in two parts, the first of which was a single-point-tool study carried out with the use of the Alcoa high-speed lathe. However, the second study, which was carried out with the use of 4-tooth solid carbide end mills in an air turbine mounted on a hydraulic shaper, proved to be more significant. For this reason the results obtained with the air turbine are presented first. Details of the set-up and cutting conditions are given in Appendix D. Most of the test results are summarized in Figs. 1-5 and in Table I.

TABLE I
WEAR TESTS ON AIR TURBINE WITH A RANGE OF CUTTER DIAMETERS*

| Test No. | Cutter Dia. (in.) | Cutting Time per Chip (μ sec) | Cutting Speed (fpm) | Feed Rate (ipm) | Feed Rate (in./tooth) | Maximum Thickness of Cut (in.) | Condition of Machined Surface | Avg Flank Wear (in.) |
|----------|-------------------|------------------------------------|---------------------|-----------------|-----------------------|--------------------------------|-------------------------------|----------------------|
| 1 | 1/4 | 242 | 1280 | 720 | .0095 | .0032 | Terrible** | .0131 |
| 2 | 1/4 | 242 | 1280 | 480 | .0065 | .0022 | Bad** | .0031 |
| 3 | 1/4 | 242 | 1280 | 240 | .0048 | .0016 | Excellent | .0027 |
| 4 | 1/4 | 242 | 1280 | 1000 | .0132 | .0045 | Terrible ⁺ | - |
| 7 | 5/16 | 214 | 1600 | 1000 | .0132 | .0045 | Excellent | .0056 |
| 10 | 5/16 | 214 | 1600 | 1200 | .016 | .0055 | Good | .0053 |
| 11 | 5/16 | 214 | 1600 | 720 | .0095 | .0032 | Good | .0035 |
| 12 | 5/16 | 214 | 1600 | 480 | .0065 | .0022 | Excellent | .0026 |
| 13 | 5/16 | 214 | 1600 | 240 | .0048 | .0016 | Excellent | .0017 |
| 8 | 3/8 | 197 | 1920 | 1000 | .0132 | .0045 | Good | .0042 |
| 9 | 1/2 | 170 | 2560 | 1000 | .0132 | .0045 | Good | .0051 |

*Each test consisted of 10 passes each 12 in. long and 0.015 in. deep. Width of cut was 0.100 in. Material A-110 titanium. Cutters: 4-tooth end mills of solid Carboly Grade 883 carbide.

**Poor finish caused by chatter.

⁺Cutter broke.

1. Air Turbine Tests

Figure 1 shows a family of lines representing the amount of wear which had been developed on the flanks of the cutting edges after different amounts of metal had been cut. These results demonstrate effectively the useful latitude of feed rates with this particular set-up, whose rigidity was severely limited by the relatively small ball bearings on the spindle of the air turbine. The consequences of operating at feeds which result in too thin a chip show up dramatically in the considerable increase in wear rate at the relatively low table feed rate of 240 ipm. At the other end of the scale, at a feed rate of 1200 ipm, the cutting action was observed to involve chatter; this chatter undoubtedly contributed to the correspondingly high wear rate observed at these conditions. It is significant that all of the available A-110 titanium alloy was cut up into chips in carrying out this particular investigation.

Further tests were carried out on both the B-120 and C-120 titanium alloys at the feed rate of 480 ipm, which had demonstrated a minimum wear rate with the A-110 alloy. It was found that the wear rates with the B-120 alloy were substantially greater than those observed with the A-110 alloy; therefore some additional tests were carried out at the slower feed rate of 240 ipm. The results for both of these speeds are plotted in Fig. 2. The B-120 alloy has consistently been the most difficult to cut of the three titanium alloys used in the tool-wear investigations. It is very probable that a higher degree of rigidity would materially reduce the observed wear rates and would shift the relative positions of the two lines in Fig. 2, since chatter occurred at the higher feed rate but did not appear to be an influential factor at the lower feed rate.

The supporting data from which the family of lines in Fig. 1 was plotted is re-plotted in Figs. 3 and 4 to show the progress of wear from the beginning to the end of each test. Figure 4 also includes the results obtained with the C-120 alloy at the feed rate of 480 ipm. It can be seen that the results are almost as good as those obtained with the A-110 alloy and are substantially better than those obtained with the B-120 alloy.

The data plotted in Figs. 1-4 represented average rates of wear for all four teeth of the individual cutters. The actual amount of wear varies from tooth to tooth depending upon the degree of run-out or eccentricity of the cutter. In addition, the actual wear land on each tooth varies in width along the tooth because of the helix angle. Consequently this too is an averaged value.

The significance and extent of these variations is illustrated in Fig. 5, which is a reproduction of original data by type. In this figure, each of the individual solid lines represents the progress of average wear as determined for each of the four individual teeth of the cutter. The shaded area, representing higher levels of wear, corresponds to the full range of the maximum

widths of wear land observed on all of the teeth. It will be noted that these levels do not deviate substantially from the averages shown by the solid lines. Thus it may be concluded that the reported wear information is a reliable indication of what can be expected at these feed rates with system rigidity at least the equivalent of that of the laboratory set-up. It can be expected, however, that improved rigidity will both reduce the rate of wear and broaden the range between minimum and maximum usable feed rates.

All of the test data shown in Figs. 1-5 were obtained with 3/8-in.-diam cutters. Actually these tests were preceded by a preliminary series wherein cutters ranging in diameter from 1/4-in. through 1/2-in. were tried at feed rates ranging from 240 ipm up to and including (in one case) 1200 ipm. All cutters were used to remove the same volume of metal, with resultant wear rates or total flank wear as summarized in Table I. The 1/4-in.-diam cutter lacked sufficient rigidity at all feed rates except at the smallest value, 240 ipm. Consequently the surface finish was marred by chatter at the higher feed rates and the cutter actually broke at the feed rate of 1000 ipm. However, these results obtained with the A-110 titanium alloy did indicate a useful latitude of cutting conditions with reasonable wear and provided the basis for the wear studies reported in Figs. 1-5.

2. Single-Point-Tool Tests

The other group of tool-wear tests was carried out with a single-point tool mounted in a Wesson holder which was mounted in the spindle of the Alcoa high-speed lathe. It was found during this series of tests that varying degrees of whipping and run-out occurred at different cutting speeds. This finding was suspected to have some influence on the wear results, and was one reason for setting up the tests with the air turbine.

In spite of the fact that the wear rates might have been exaggerated by the spindle run-out, the results confirmed the original premise that high cutting speeds can be tolerated if the tooth-contact time is sufficiently short. Satisfactory cutting was accomplished over a broad range of speeds and with feed rates expressed in inches per tooth (ipt). It is significant that feed rates were carried up to .062 ipt. Had feed rates of this order of magnitude been possible with the air turbine, they would have gone as high as 5000 ipm. This is further support for the contention that increased rigidity broadens the latitude of useful feed rates and extends them far beyond anything possible with existing machine tools.

Wear data obtained with single-point tools when cutting the A-110 titanium alloy are summarized for variable speed and variable feed rate in Tables II and III, respectively.

In summarizing and interpreting the tool wear results it is important to emphasize two things. First is the fact that tool wear is gradual and not

TABLE II

SINGLE-TOOTH CUTTER WEAR: VARIABLE SPEED

| Cutting Speed (fpm) | Volume | | Maximum Cut Thickness (in.) | Cutting Time per Chip (μ sec) | Average Landwear (in.) |
|---------------------|---|-----------------|-----------------------------|------------------------------------|------------------------|
| | Removal Rate in. $\bar{3}$ /min/in. of Cutting Edge | Feed Rate (ipm) | | | |
| 700 | 0.588 | 38.6 | 0.0041 | 179 | 0.0028 |
| 700 | 1.150 | 77.0 | 0.0082 | 1000 | 0.0042 |
| 1033 | 0.588 | 38.6 | 0.0027 | 119 | 0.0025 |
| 1033 | 0.870 | 57.9 | 0.0041 | 184 | 0.0035 |
| 1375 | 0.588 | 38.6 | 0.0020 | 92 | 0.0015 |
| 1375 | 0.870 | 57.9 | 0.0031 | 138 | 0.0062 |
| 1375 | 1.150 | 77.0 | 0.0041 | 500 | 0.0030 |
| 1375 | 2.310 | 154.0 | 0.0082 | 500 | 0.0104 |
| 1718 | 0.588 | 38.6 | 0.0016 | 72 | 0.0014 |
| 1718 | 0.870 | 57.9 | 0.0024 | 110 | 0.0050 |
| 1718 | 1.150 | 77.0 | 0.0033 | 417 | 0.0100 |
| 2061 | 0.588 | 38.6 | 0.0013 | 60 | 0.0012 |
| 2061 | 0.870 | 57.9 | 0.0020 | 92 | 0.0058 |
| 2061 | 1.150 | 77.0 | 0.0027 | 333 | 0.0046 |
| 2061 | 1.730 | 116.0 | 0.0041 | 333 | 0.0130 |

TABLE III

SINGLE-TOOTH CUTTER WEAR: VARIABLE FEED RATE

| Cutting Speed (fpm) | Volume | | Maximum Cut Thickness (in.) | Cutting Time per Chip (μ sec) | Average Landwear (in.) |
|---------------------|---|-----------------|-----------------------------|------------------------------------|------------------------|
| | Removal Rate in. $\bar{3}$ /min/in. of Cutting Edge | Feed Rate (ipm) | | | |
| 700 | 0.588 | 38.6 | 0.0041 | 179 | 0.0028 |
| 1033 | 0.588 | 38.6 | 0.0027 | 119 | 0.0025 |
| 1375 | 0.588 | 38.6 | 0.0020 | 92 | 0.0015 |
| 1718 | 0.588 | 38.6 | 0.0016 | 72 | 0.0014 |
| 2061 | 0.588 | 38.6 | 0.0013 | 60 | 0.0012 |
| 1033 | 0.870 | 57.9 | 0.0041 | 184 | 0.0035 |
| 1375 | 0.870 | 57.9 | 0.0031 | 138 | 0.0062 |
| 1718 | 0.870 | 57.9 | 0.0024 | 110 | 0.0050 |
| 2061 | 0.870 | 57.9 | 0.0020 | 92 | 0.0058 |
| 700 | 1.150 | 77.0 | 0.0082 | 1000 | 0.0042 |
| 1033 | 1.150 | 77.0 | 0.0054 | 750 | 0.0054 |
| 1375 | 1.150 | 77.0 | 0.0041 | 500 | 0.0030 |
| 1718 | 1.150 | 77.0 | 0.0033 | 417 | 0.0100 |
| 2061 | 1.150 | 77.0 | 0.0027 | 333 | 0.0046 |
| 1375 | 2.31 | 154.0 | 0.0082 | 500 | 0.0104 |
| 2061 | 1.73 | 116.0 | 0.0041 | 333 | 0.0130 |

catastrophic. Therefore, the wear rate is predictable and total wear is subject to control. Second, it is evident that the total number of cubic inches of metal cut per tool re-grind is somewhat less than can be obtained at considerably lower cutting speeds. Even if tool wear for a given volume of metal were somewhat increased at the very high cutting speeds, the rate of metal removal would be greatly increased over the rate at present commercial speeds; and therefore it would still be economical to re-sharpen cutters more frequently (if necessary) in order to gain the advantages of more rapid metal removal.

B. CUTTING-TEMPERATURE STUDIES

Cutting-temperature studies were carried out by two different methods. In one method, a shielded thermocouple imbedded in the cutting tool itself is used. This method, of course, yields information only on temperature at the tip of the thermocouple and not on the maximum temperature which occurs at the tool-chip interface. But even though the recorded temperature values are much lower, they reflect both qualitatively and quantitatively the conditions at the cutting edge. In the other method, a lead sulfide cell was used to measure the radiation from the tool flank immediately after it came out of a cut. This method yielded much higher temperature readings, as expected, but it was found that the qualitative characteristics shown by both approaches were the same.

1. Tests With Imbedded Thermocouple

Typical results obtained with the imbedded thermocouple are given in Figs. 6-12. Figure 6 shows the variation of temperatures over a range of feed rates while cutting C-1018 steel and A-110 titanium at a constant cutting speed of 3000 fpm. It is obvious that a chip thickness of 0.001 in. is entirely too thin for milling the titanium alloy. Moreover, it is apparent that the onset of chip segmentation does indeed reduce temperature appreciably with the titanium and to such an extent that the temperatures are not only comparable but slightly below those for the steel at the larger feed rates.

Similar data for a cutting speed of 1500 fpm are shown in Fig. 7. At this speed the temperatures measured in cutting steel are considerably lower than those measured in cutting the titanium. This can be explained by the fact that the steel is far less sensitive to chip segmentation created by the standing waves which occur at the higher cutting speeds; consequently, the temperatures measured in cutting the steel increased substantially as the cutting speed was doubled.

It is also significant that temperatures for A-110 titanium at chip thicknesses from 0.002 to 0.008 in. were not appreciably greater at the higher cutting speeds. This can be attributed to the high degree of chip segmenta-

tion which can be achieved with titanium alloys.

Figures 10, 11, and 12 show reproductions of the actual chart records on which the temperatures indicated by the imbedded thermocouples were recorded. The charts in Fig. 10 show the results obtained at 3000 fpm cutting speed and at feeds of 0.001 and 0.008 ipt for both the steel and the titanium. It is obvious from these charts that at the lighter cut of 0.001, the temperature for the titanium is very much higher than that for the steel. At the heavier feed rate of 0.008, on the other hand, it drops below that for the steel.

The charts in Figs. 11 and 12 for a cutting speed of 1500 fpm at feeds of 0.001 and 0.008 ipt, respectively, show that even the steel is sensitive to thin cuts at the low speeds, and that the temperature fails to drop off significantly at the lighter cut. It should be remembered in evaluating the results shown in Figs. 11 and 12 that the differences in rate of metal removal and in total amount of metal cut have the same ratio (1:8) as the differences between chip thicknesses of 0.001 and 0.008. This is dramatic evidence of the role of segmentation in reducing the total energy required for cutting.

2. Tests With Lead Sulfide Cell

Data obtained from tests with the lead sulfide cell wherein the temperatures were indicated by radiation from the flank of the tool are plotted in Figs. 13-20. Qualitatively the results are identical to those obtained with the imbedded thermocouple. They differ only in that the increase in cutting temperature associated with too thin a cut appears somewhat earlier in terms of chip thickness; that is, the peak temperature for the titanium alloys at thin cuts appears to occur at chip thicknesses of about 0.002 in. rather than at the 0.001-in. thicknesses for the chip-tool interface indicated by the imbedded thermocouple. Also, it is evident that chip segmentation exerts a depressing influence on the temperatures with increased thickness of chip although this influence is not as pronounced on the tool flank as at the chip-tool interface.

It is quite clear from the plots of temperature versus cutting time in Figs. 13-20 that cutting temperature can increase very rapidly with increased length of cutting time unless substantial chip segmentation develops. Furthermore, it is clear that effective segmentation occurs more readily at thicker cuts with each work material, and more readily with titanium than with ferrous metals.

C. STUDIES OF FORCES, STANDING WAVES, AND CHIP SEGMENTATION

Some additional information was obtained on the relationship of standing waves to forces and chip segmentation. The results of these studies are reported briefly Figs. 21-23.

Figure 21 shows oscilloscope records of the internal vibrations of a titanium A-110 test specimen as indicated by semiconductor strain gages mounted directly on the specimen. A cut was made at a speed of 2250 fpm and a feed rate or chip thickness of 0.008 in. The record shown in Fig. 21(a) was obtained when the bar was 10 in. long; that shown in Fig. 21(b) was obtained for a tuned length of 3-1/2 in. It will be noted that at the beginning of the cut the vibrations were very much stronger with the tuned bar than they were with the longer bar.

Figure 22 shows typical oscilloscope records for the tangential cutting force and the internal vibrations of a test specimen. In this case brass was being cut at speeds of 1500 and 7500 fpm. It will be noted in Fig. 22(a) that the cutting force increased to a peak and then decreased to a considerably lower level after the standing waves became strong enough to produce continued segmentation in the chip. The steady-state cutting force was reduced to less than 15% of the peak value as a result of segmentation. This is typical also of the observations for titanium. The oscilloscope record in Fig. 22(b) shows a trace made at a higher sweep frequency, at which the cutting force had not yet appeared because of the mass attenuation. This record shows strong internal oscillations at approximately 140 kc despite the fact that the test specimen was 10 in. long and essentially untuned—although the clamp was 7/8-in. from the working end, which would encourage the third harmonic of the fundamental. The significance of this result lies in the indication that a workpiece can vibrate at a very high harmonic of the fundamental frequency. This means that standing waves at very high frequency can occur in even very large workpieces where the physical dimensions would dictate considerably lower fundamental frequencies. Brass segments much more readily than titanium, which explains the greater importance of tuning in the case of titanium.

The three oscilloscope records in Fig. 23 illustrate two additional behavior characteristics of interest. A comparison of records (a) and (b) shows that the weaker tendency for segmentation with aluminum causes the reduction in cutting force to be only about 60%. On the other hand, segmentation in the brass was so sharp that the segmentation frequency appeared in the force record. A comparison of the two records for brass at (b) and (c) shows that the very short cutting time at the cutting speed of 7500 fpm did not provide sufficient time for a standing wave to develop to an effective level. The specimens were clamped 2 in. from the working ends, which explains the contrast with the results shown in Fig. 22. Clamping at the point tended to inhibit the third harmonic. Thus, in general, one must expect the beneficial effects of higher cutting speeds resulting from segmentation to disappear under certain conditions. This would not eliminate the favorable, time-dependent temperature effects at high speeds, but the temperatures would be proportionately higher because of the greater energy requirements.

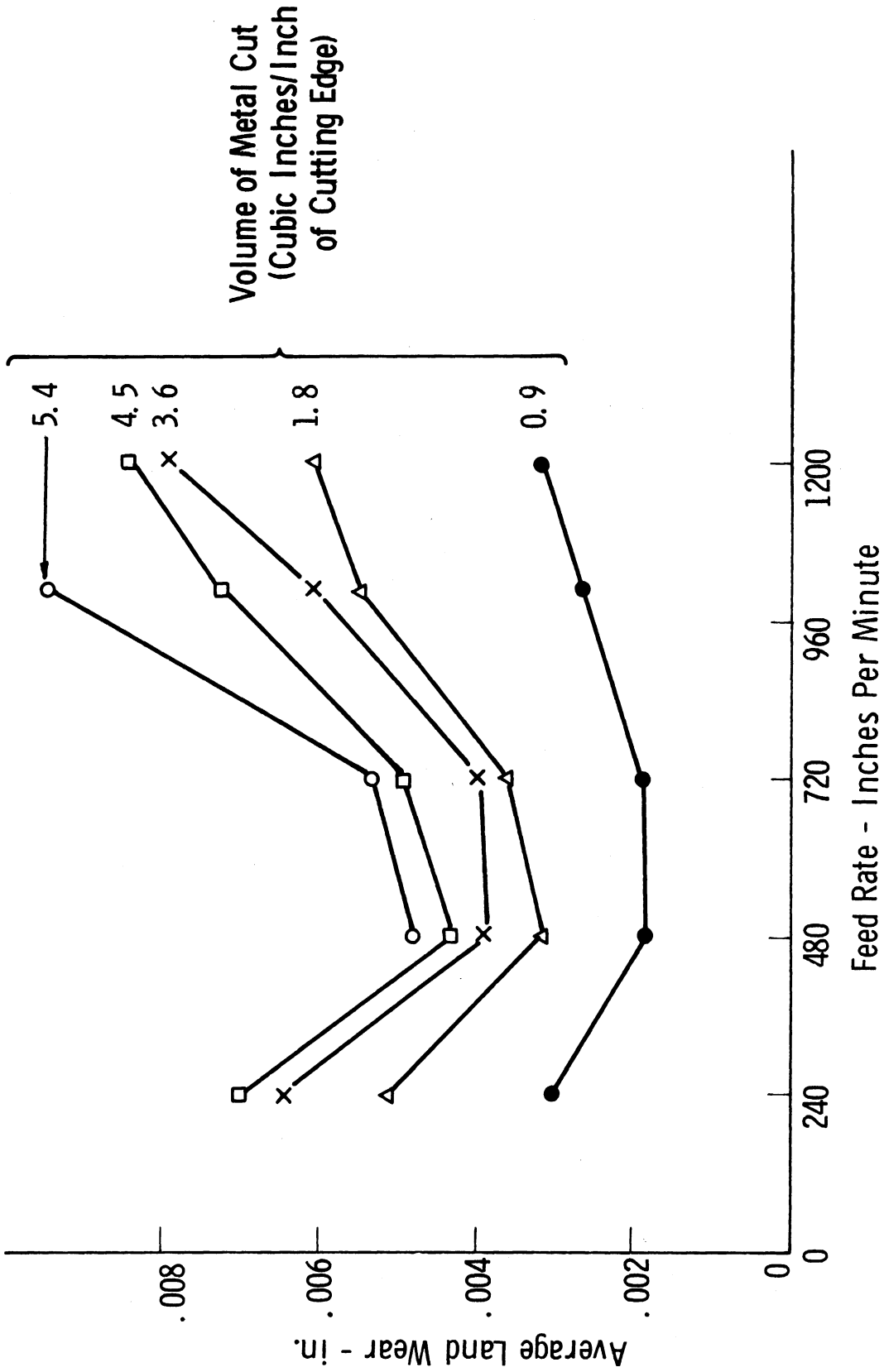


Fig. 1. Tool wear vs. feed rate (A-110 titanium). Average land wear for 3/8-in.-diam, 4-tooth solid carbide (C-2) end mills operated at an average of 19,000 rpm or 1920 fpm. Maximum chip thickness varied from 0.0015 in. to 0.0055 in. Cutting time per chip averaged 200 usec. Workpiece test section was 0.100 in. wide by 12 in. long. All cuts were climb milling at a depth of 0.015 in.

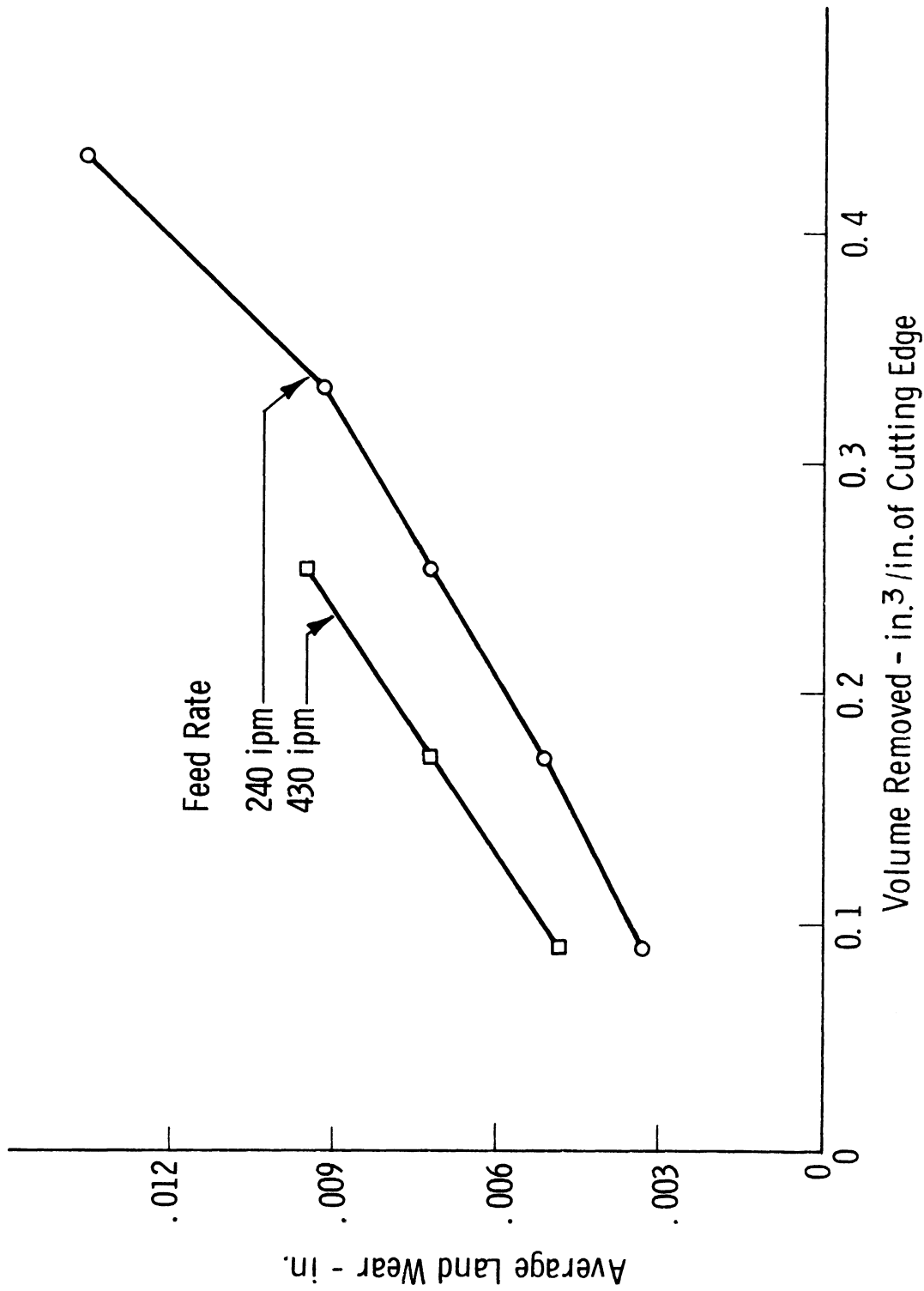


Fig. 2. Tool wear vs. volume of metal cut (B-120 titanium). High-speed milling with 3/8-in.-diam, 4-tooth carbide end mill at constant depth of cut and cutting speed. Note orderly progression of wear with time and amount of metal cut. Maximum chip thicknesses were 0.0015 in. and 0.0022 in. Workpiece size same as in Fig. 1.

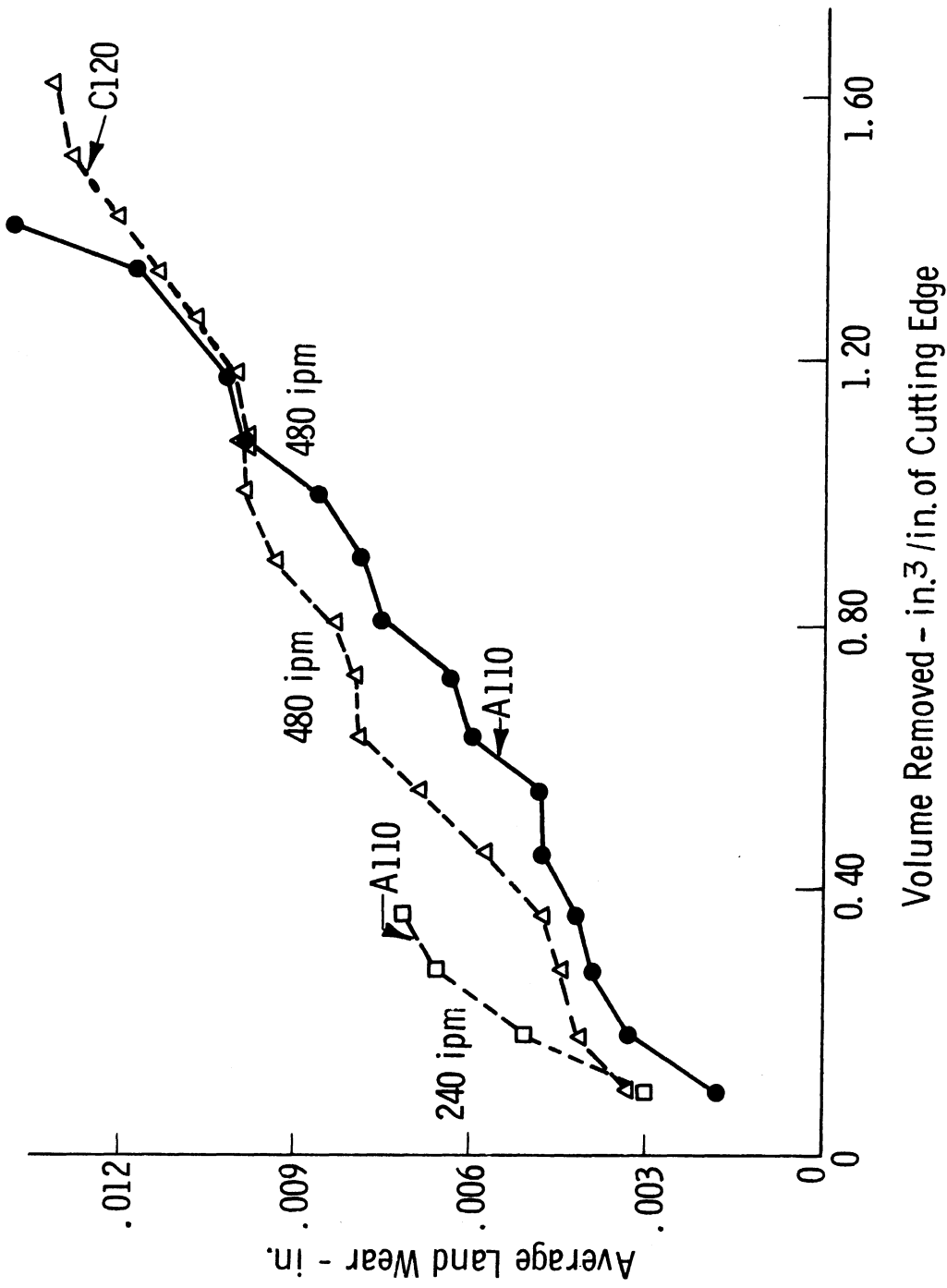


Fig. 3. Tool wear vs. volume of metal cut (A-110 and C-120 titanium). Cutting conditions same as in Fig. 2. Note that grade C-120 titanium cuts almost as readily as grade A-110. Volume cut for the same tool wear is 4 times that for B-120 shown in Fig. 2.

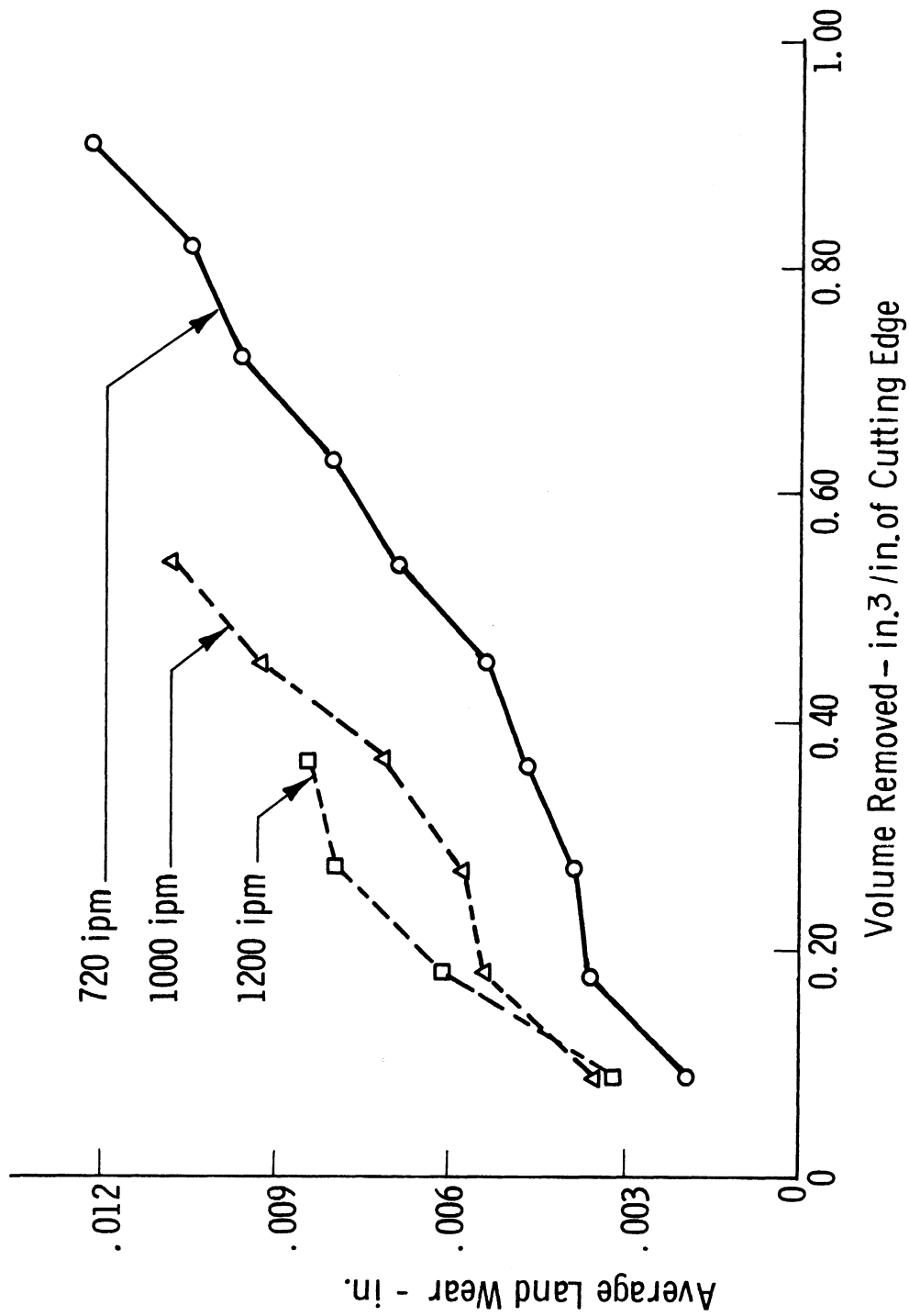


Fig. 4. Tool wear vs. volume of metal cut (A-110 titanium). Cutting conditions same as in Figs. 2 and 3 except that feed rates are higher. Note that wear rate at 720 ipm is not appreciably greater than at 480 ipm shown in Fig. 3.

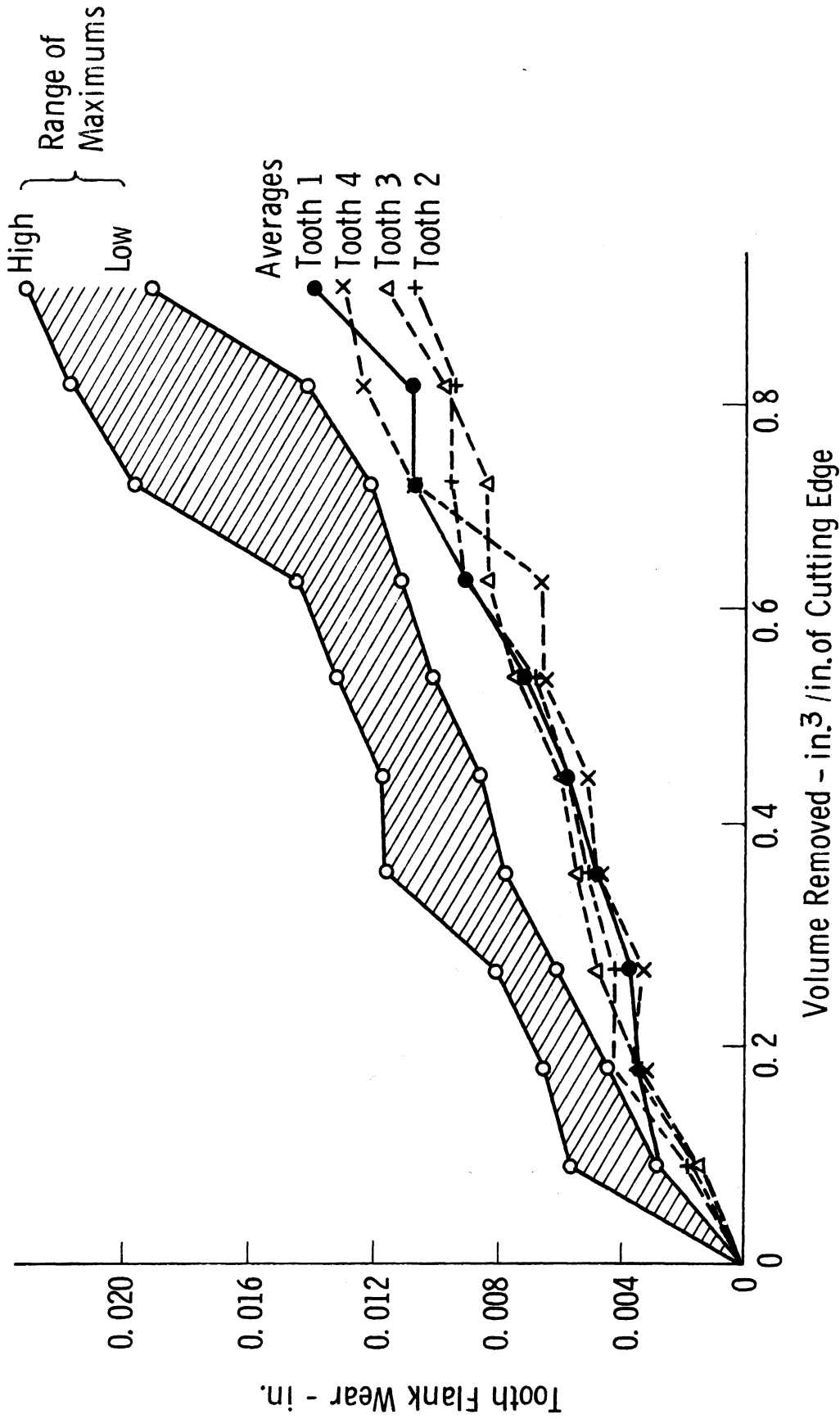


Fig. 5. Wear vs. volume removed (A-110 titanium). Shows range of measured wear values for A-110 titanium milled with $3/8$ -in.-diam carbide cutter at a cutting speed of 1920 fpm and a feed rate of 720 ipm. Maximum wear at any point on the cutter seldom exceeded twice the average for all teeth. This was typical for all tests carried out with the air turbine.

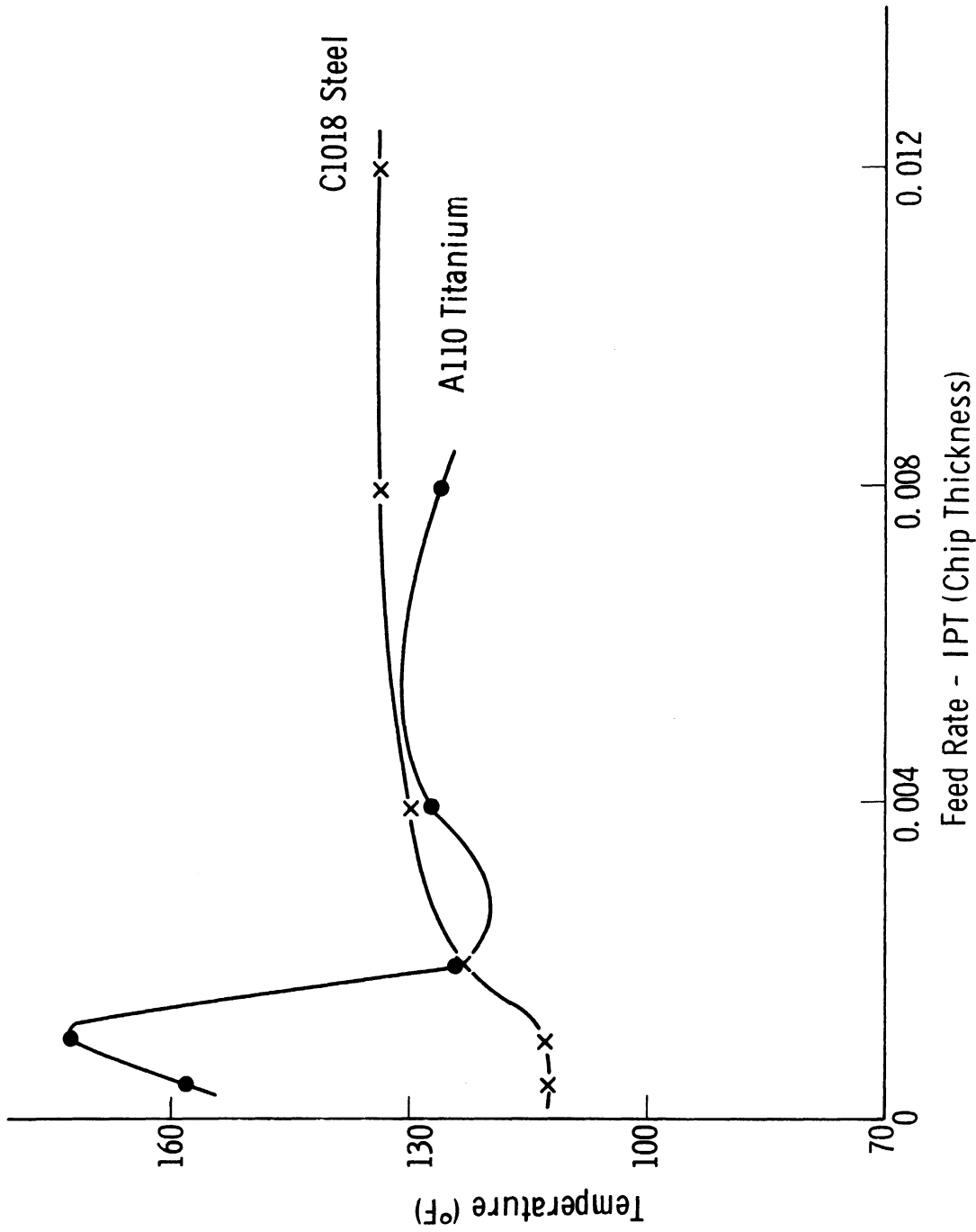


Fig. 6. Tool temperature at imbedded thermocouple (3000 fpm). Maximum temperatures indicated by chart records of the type shown in Figs. 10 to 12. Four cuts 1/2-in. long by 0.100-in. wide were made for each test. Carbide tools contained a thermocouple imbedded as shown in Fig. A-6 (Appendix A). Total cut duration was 0.12 sec; cutting time for each chip was 835 μ sec.

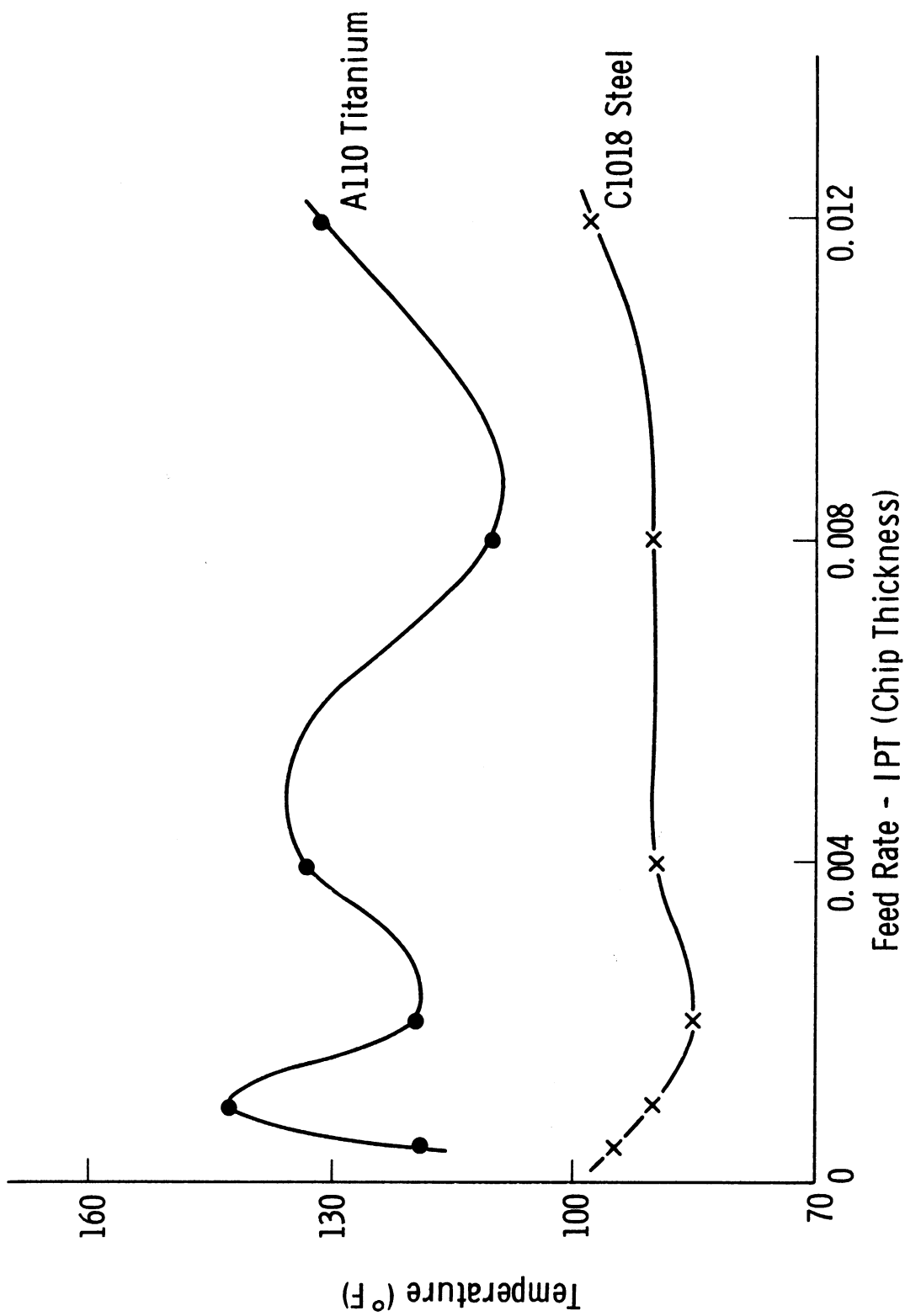


Fig. 7. Tool temperature at imbedded thermocouple (1500 fpm). Test conditions same as for Fig. 6 except for fpm rates.

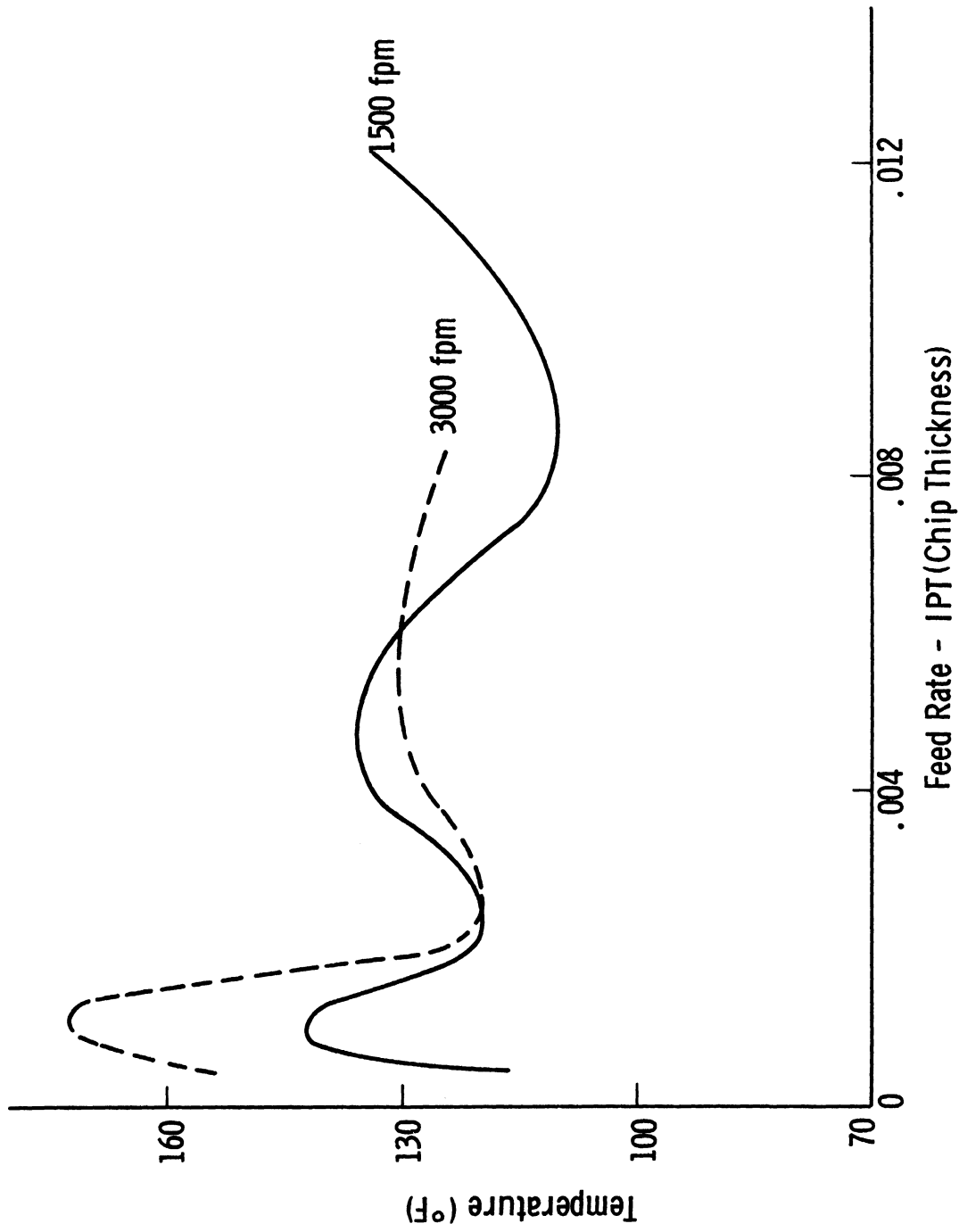


Fig. 8. Tool temperature at imbedded thermocouple (A-110 titanium). A comparison of the curves for A-110 titanium replotted from Figs. 6 and 7.

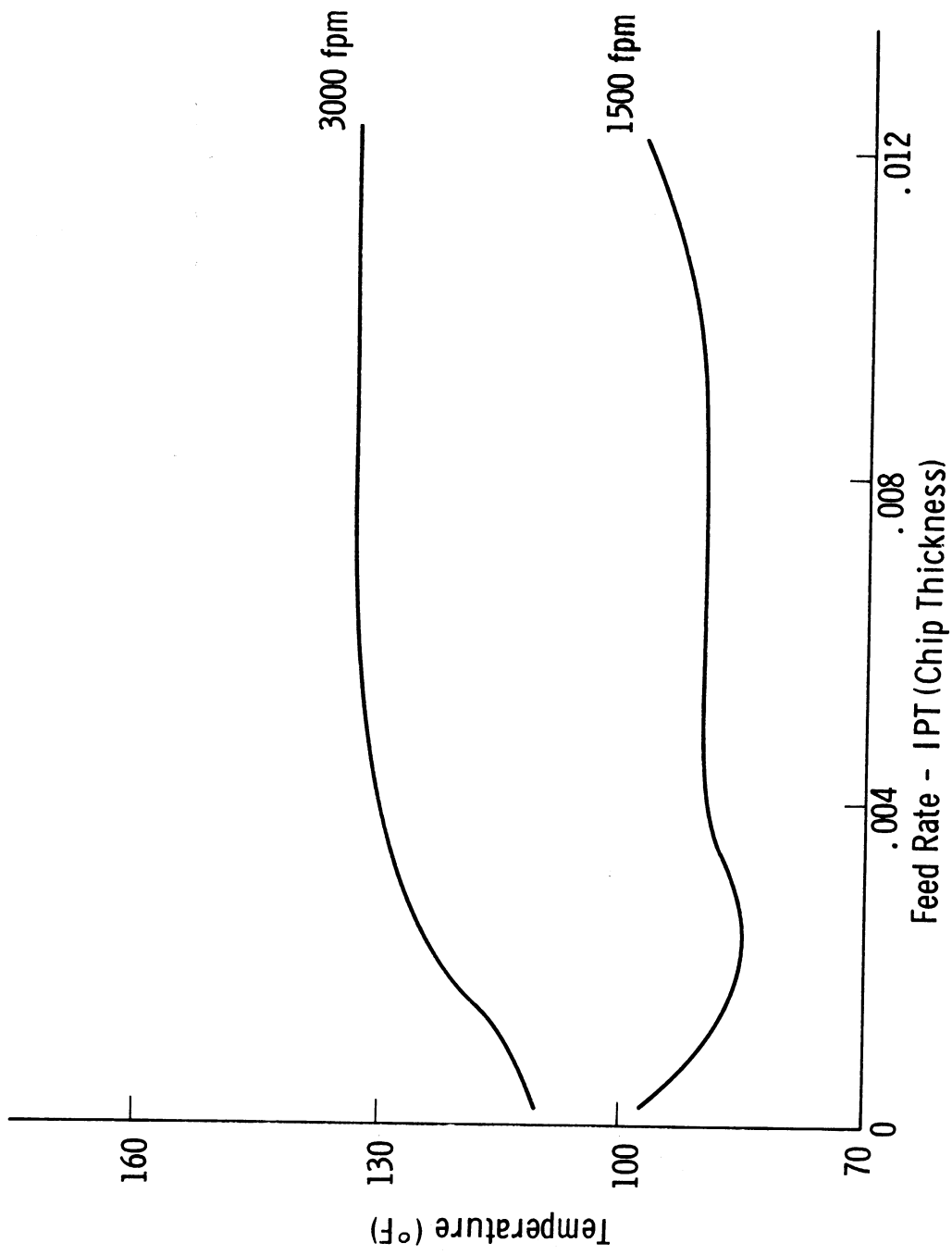


Fig. 9. Tool temperature at imbedded thermocouple (C-1018 steel). A comparison of the curves for C-1018 steel replotted from Figs. 6 and 7.

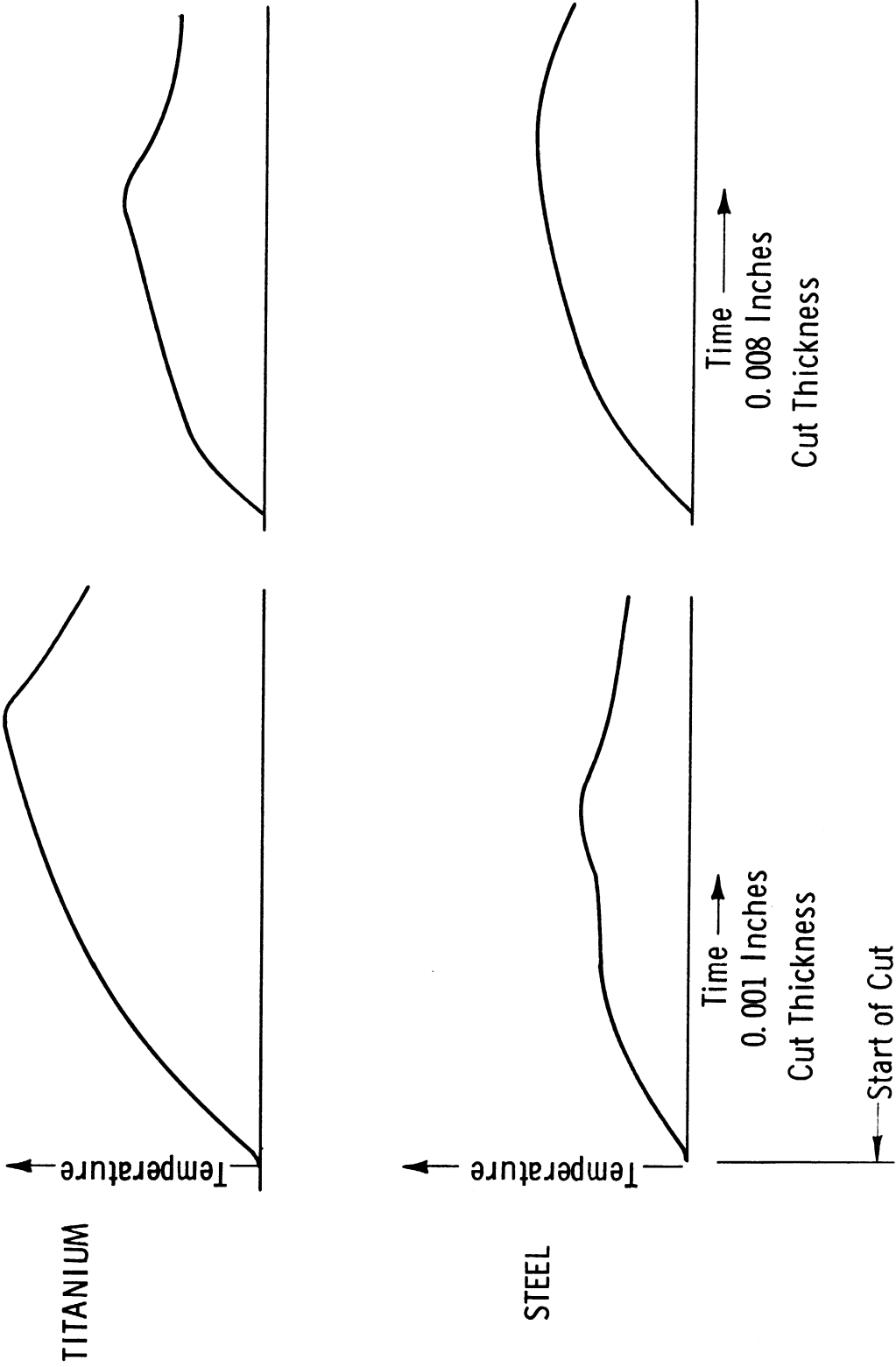


Fig. 10. Tool temperature at imbedded thermocouple (original chart records). Note that increased cut thickness actually decreases temperature when cutting A-110 titanium but increases the temperature for C-1018 steel. Cutting conditions same as for Fig. 6. All charts made at the same sensitivity of 500 $\mu\text{v}/\text{cm}$. Cutting speed 3000 fpm.

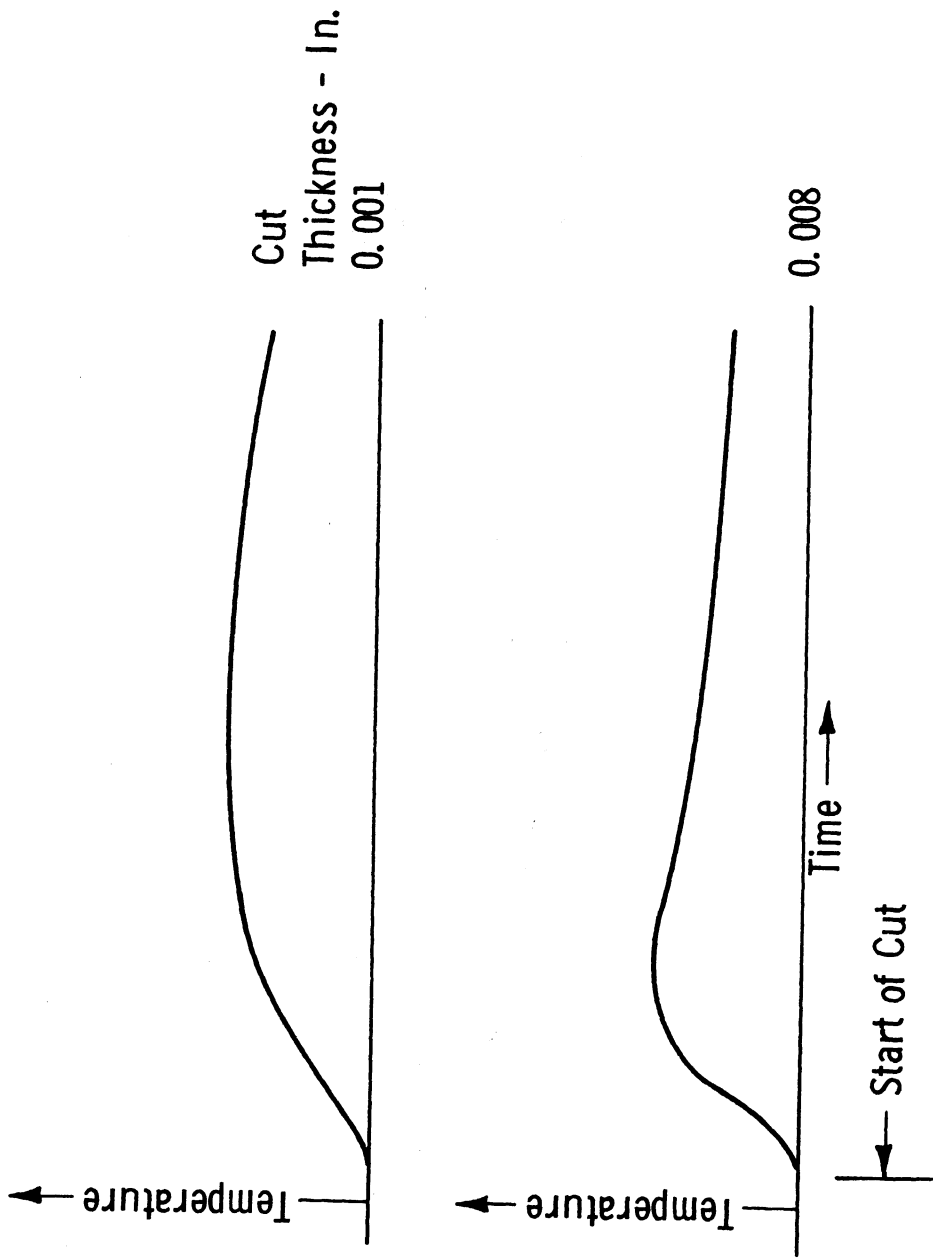


Fig. 11. Tool temperature at imbedded thermocouple (records for C-1018 steel). Cutting speed 1500 fpm. Note the rapid drop in temperature for the cut at 0.008-in. thickness compared to that for the lighter cut of 0.0001-in. Sensitivity for both records was 200 $\mu\text{v}/\text{cm}$, indicating a pronounced influence of chip segmentation at the heavier cuts even with steel.

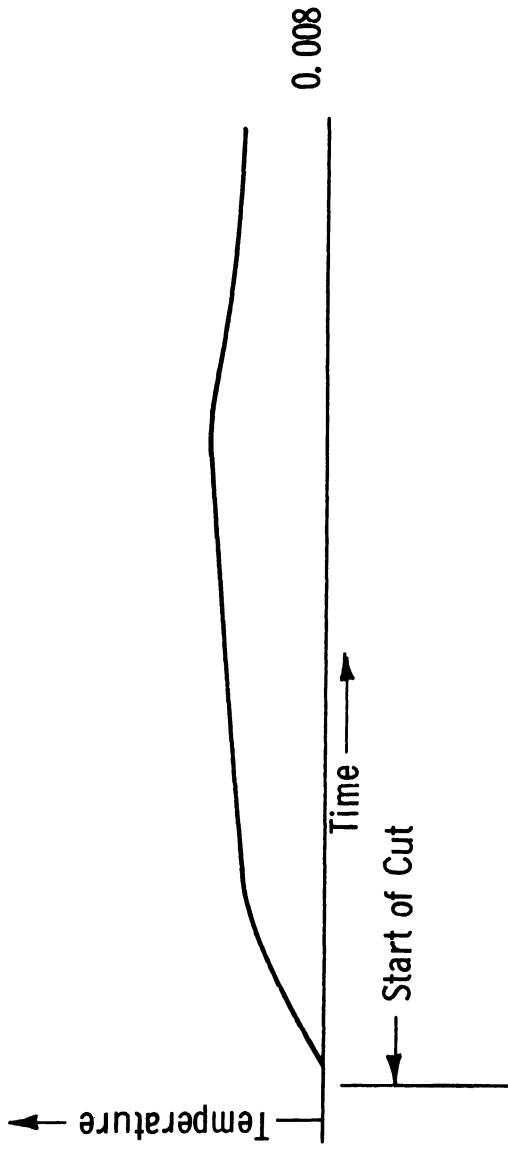
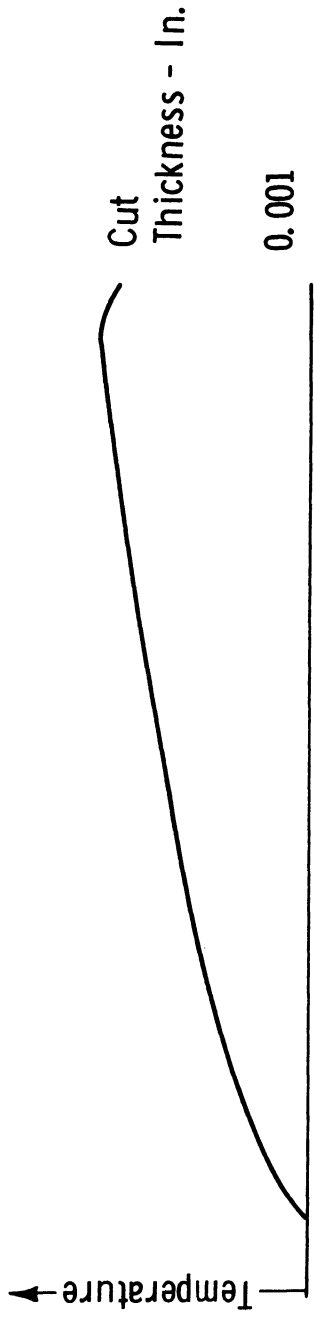


Fig. 12. Tool temperature at imbedded thermocouple (records for A-l10 titanium). Cutting conditions same as Fig. 11. Voltage sensitivity 500 $\mu\text{v}/\text{cm}$.

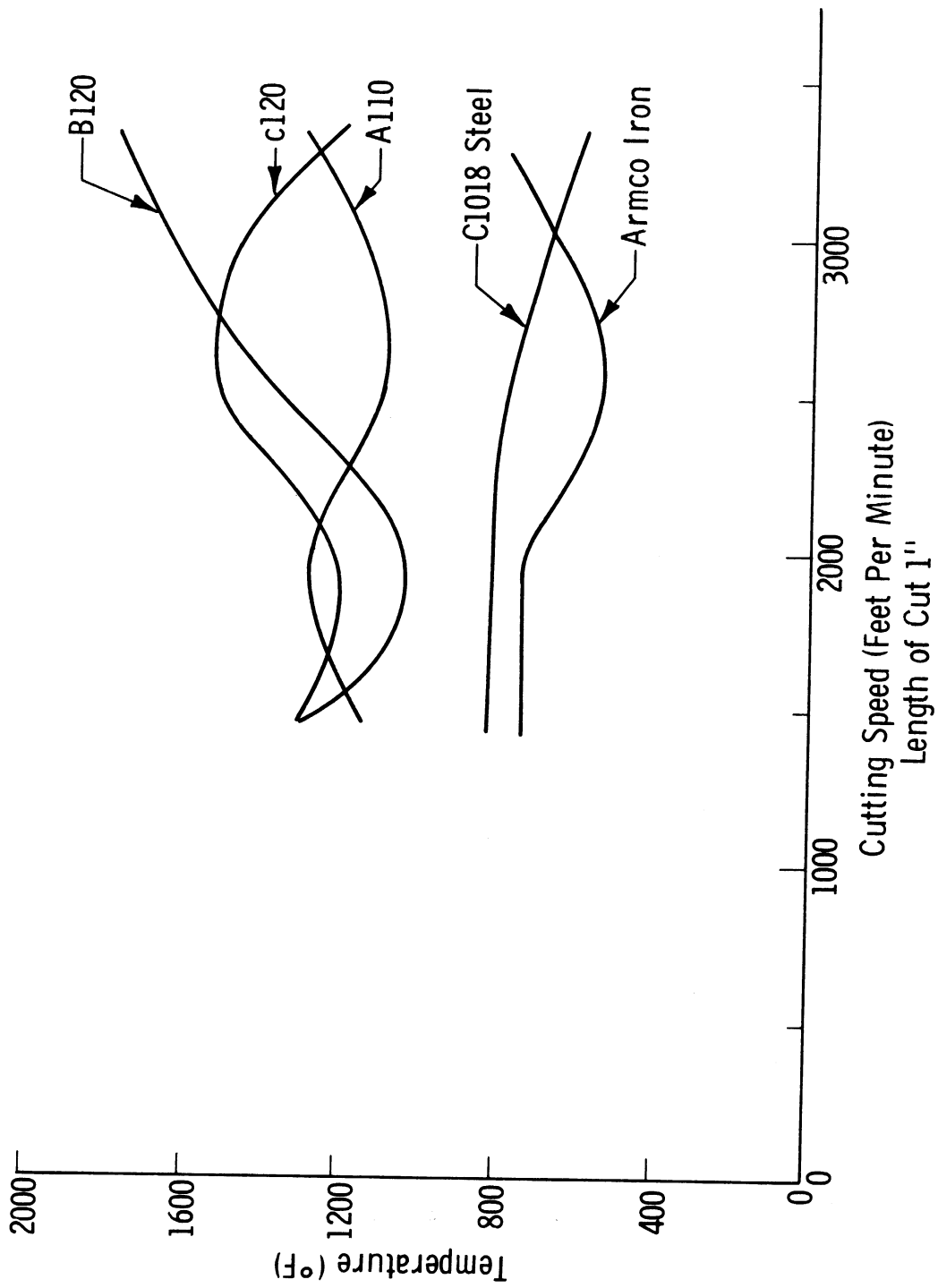


Fig. 13. Tool-flank temperature vs. cutting speed for five different metals. Data obtained with lead sulfide cell in a set-up illustrated in Fig. A-1 (Appendix A). All cuts 1 in. long at a thickness of 0.002 in. Cutting time per chip varied from 0.97 to 3.2 msec.

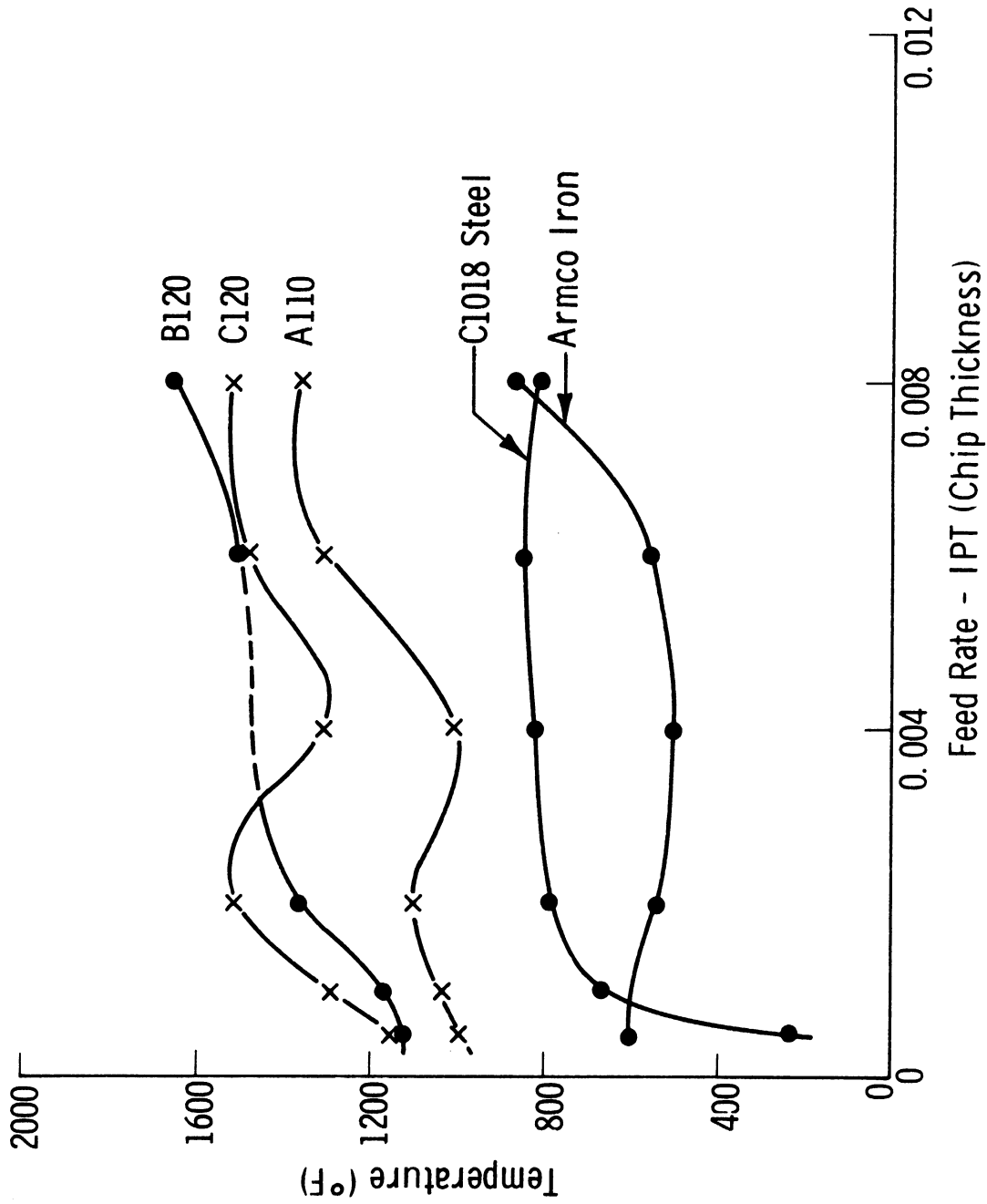


Fig. 14. Tool-flank temperature vs. cut thickness for five different metals. Data obtained at constant cutting speed of 2500 fpm. Length of cut constant at 1 in. Cutting time per chip 1.86 msec. Tool material: C-2 carbide.

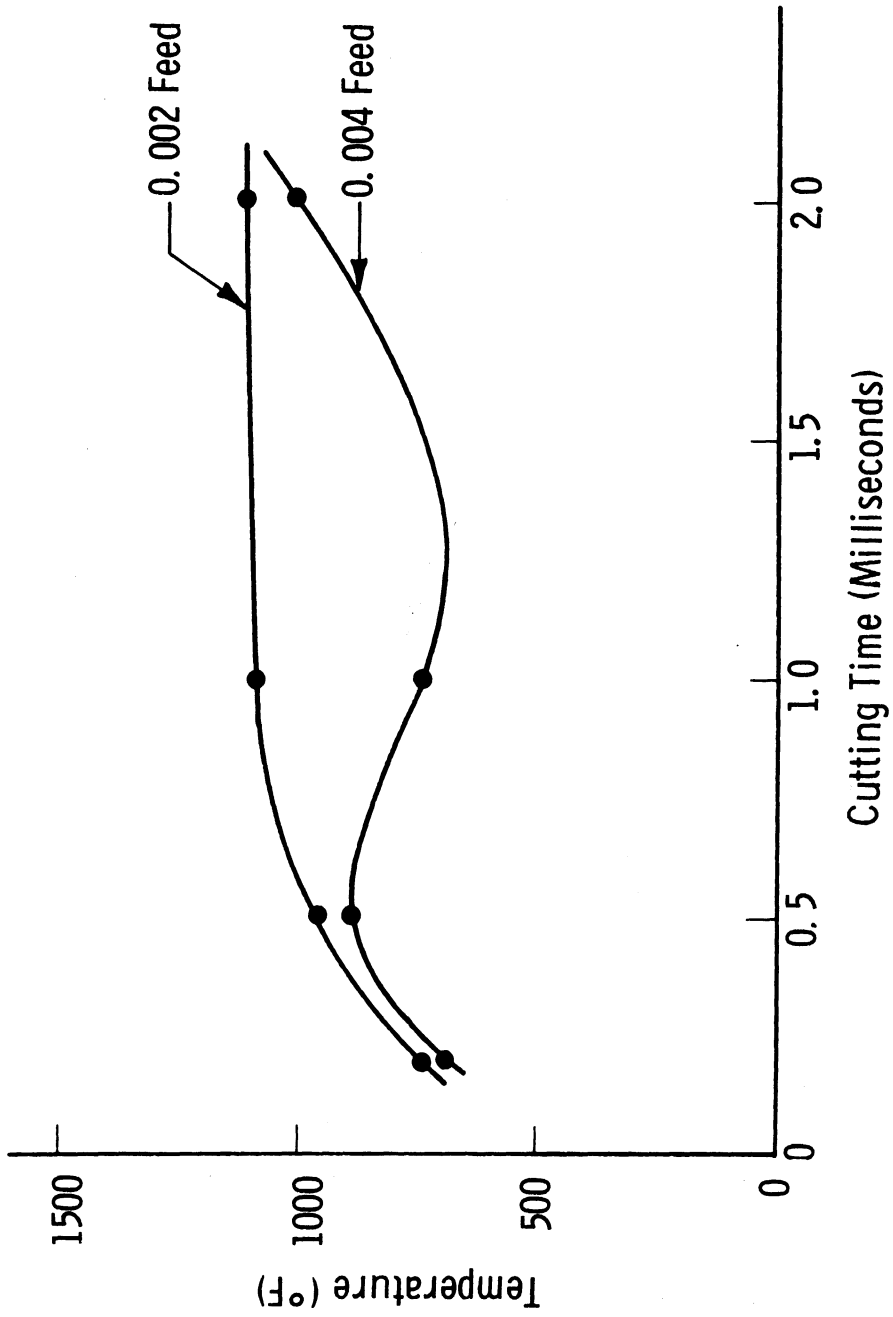


Fig. 15. Tool-flank temperature vs. cutting time (A-110 titanium). Data obtained at constant cutting speed of 2500 fpm. Cut thickness or feed as indicated.

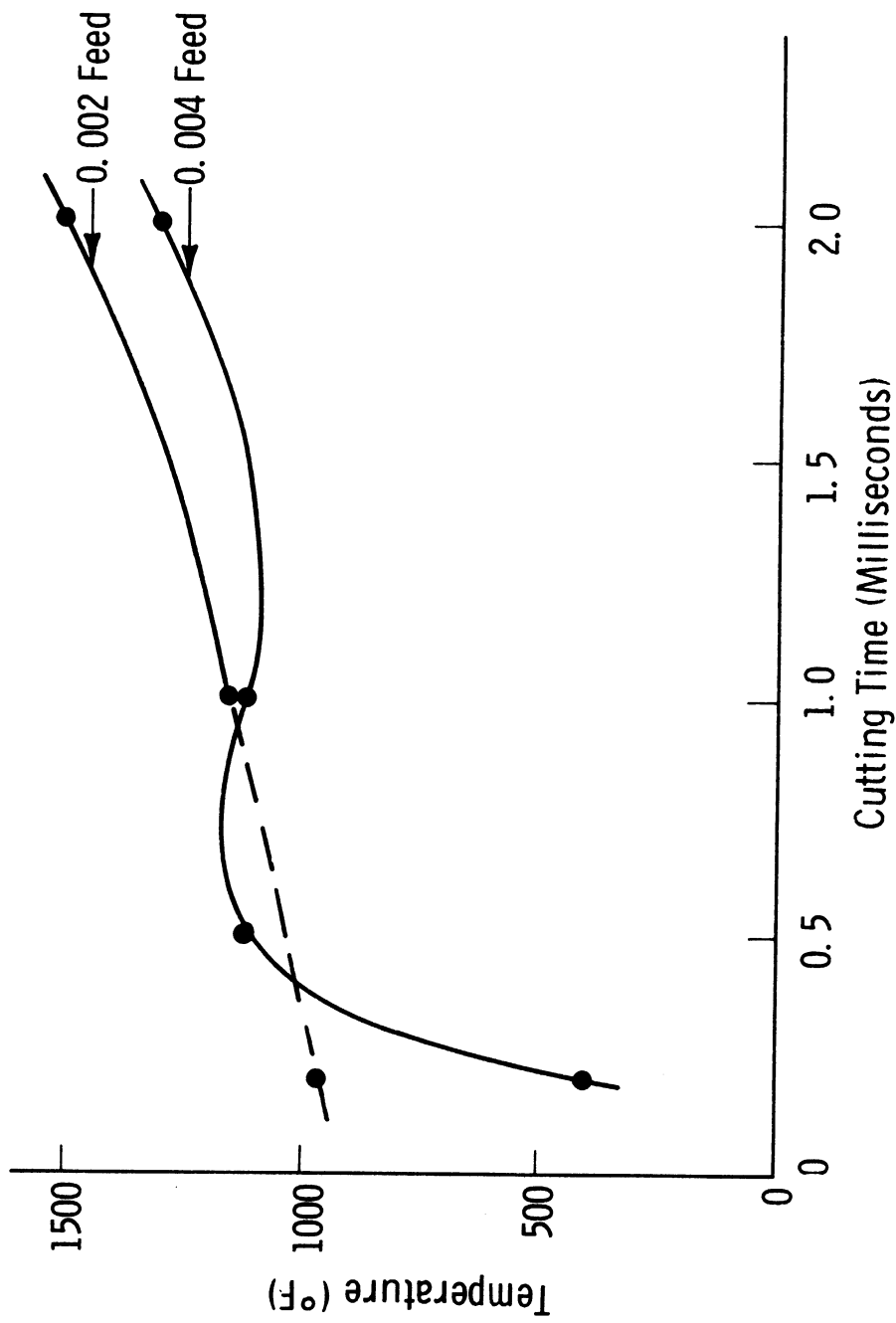


Fig. 16. Tool-flank temperature vs. cutting time (C-120 titanium). Test conditions same as for Fig. 15.

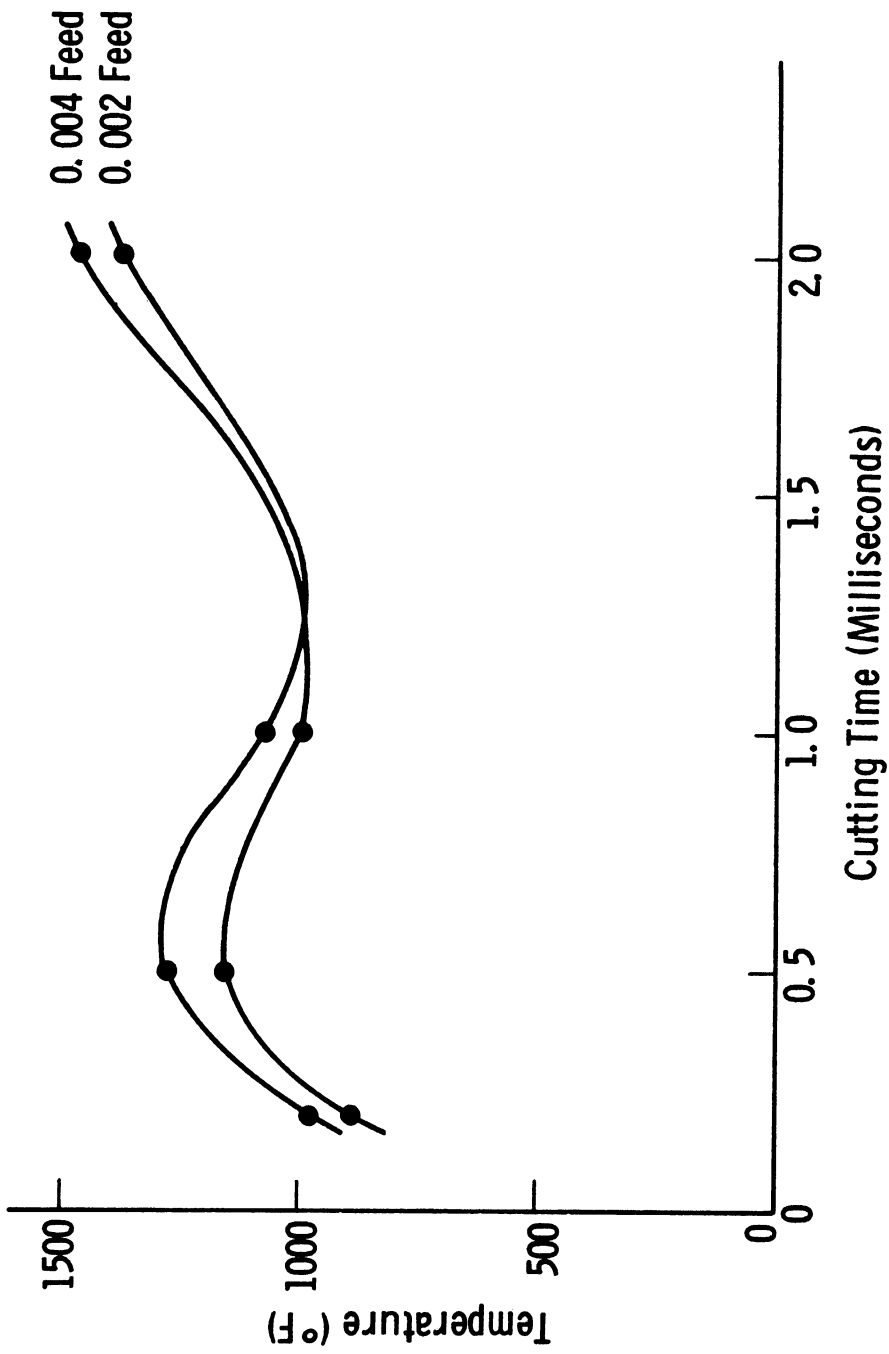


Fig. 17. Tool-flank temperature vs. cutting time (B-120 titanium). Test conditions same as for Fig. 15.

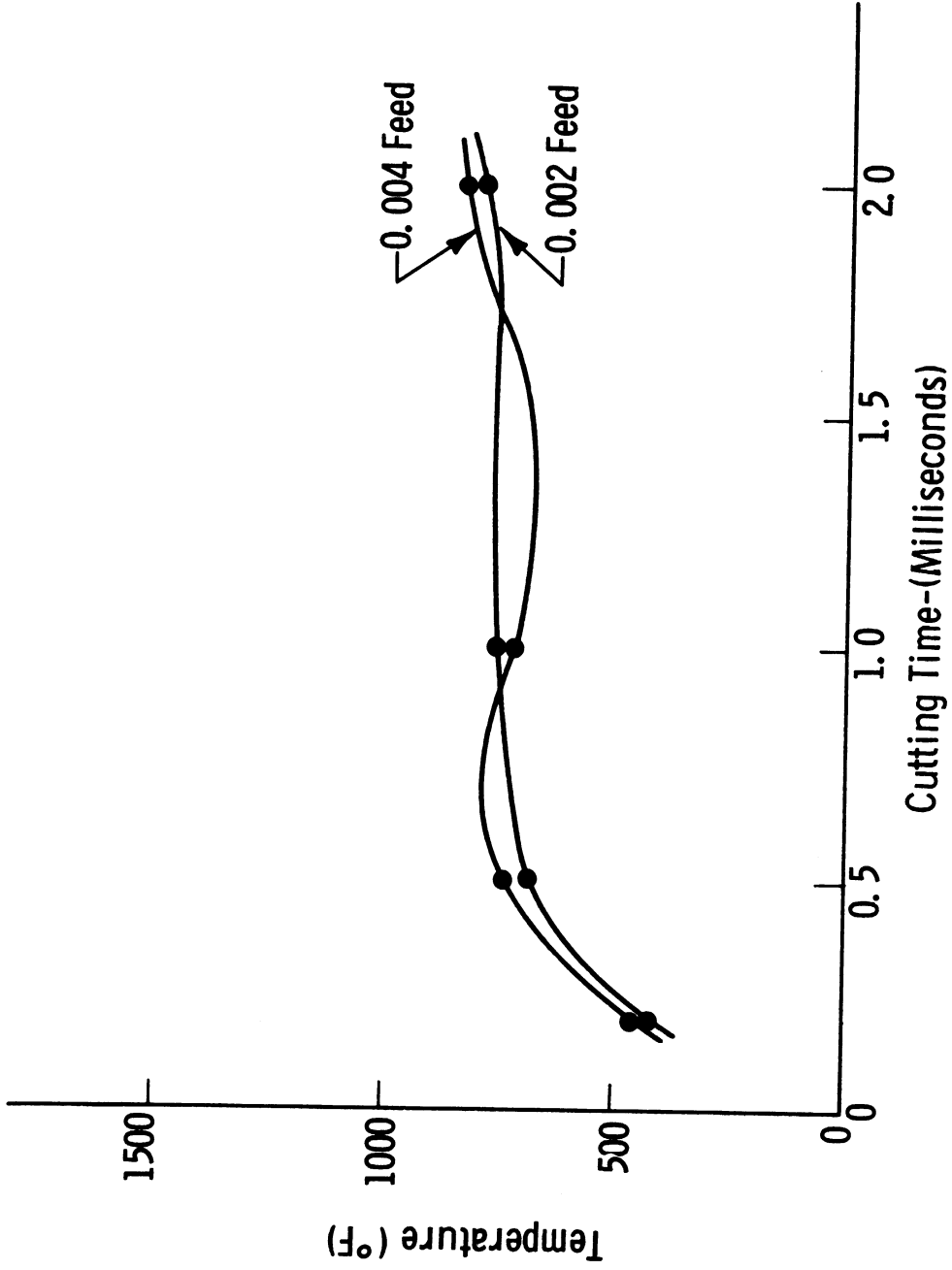


Fig. 18. Tool-flank temperature vs. cutting time (C-1018 steel). Test conditions same as for Fig. 15.

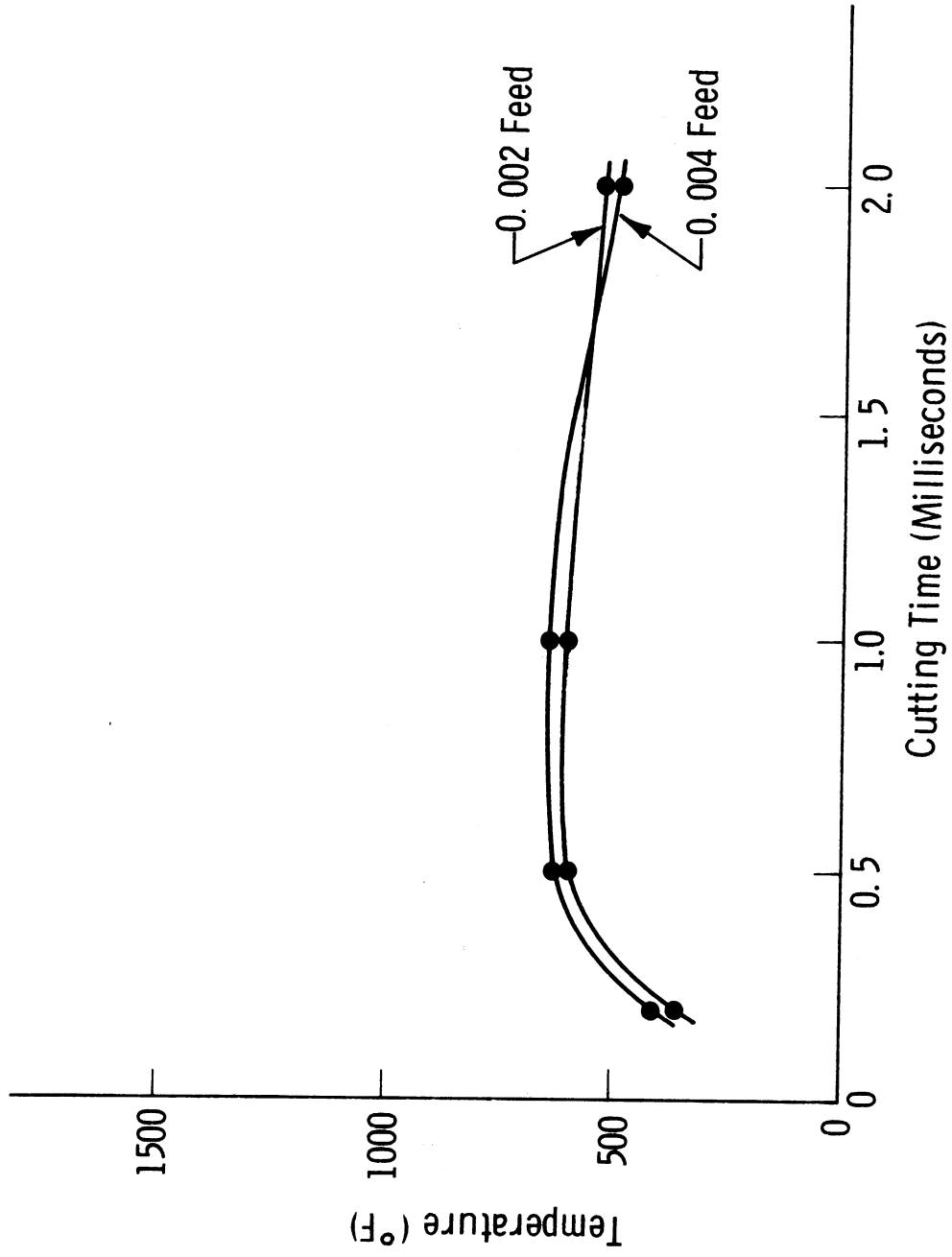


Fig. 19. Tool-flank temperature vs. cutting time (Armco iron). Test conditions same as for Fig. 15.

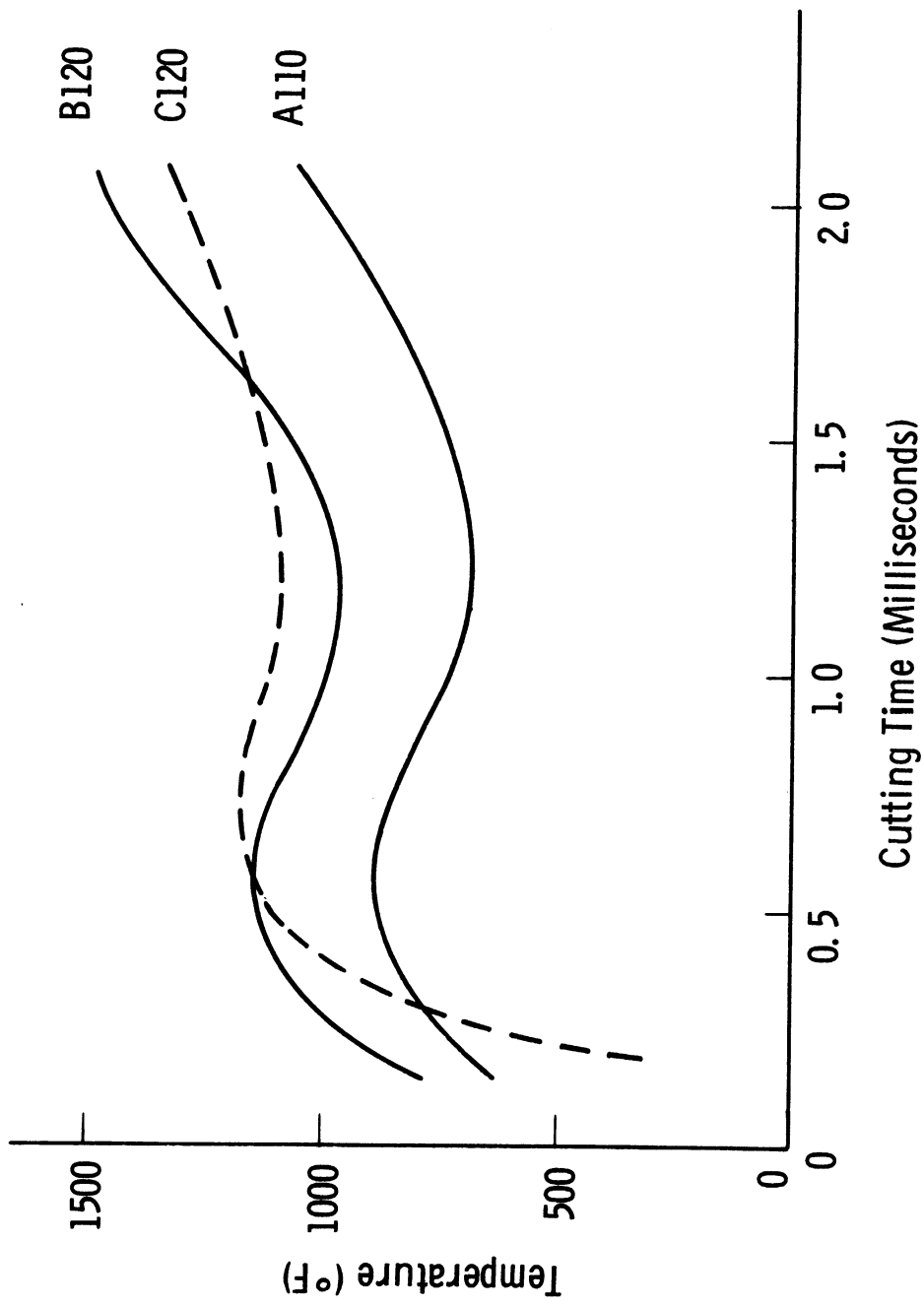
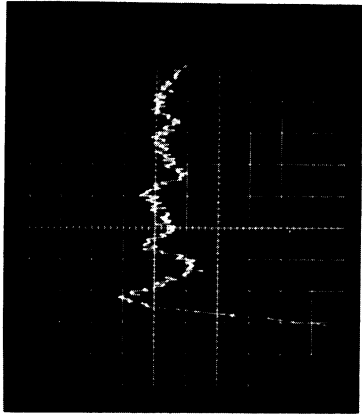


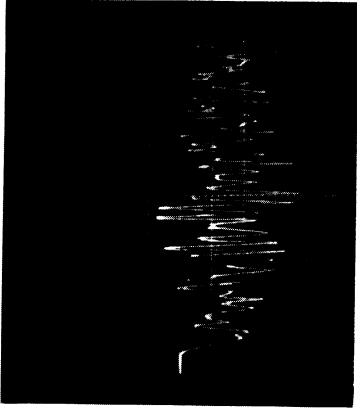
Fig. 20. Comparison of three grades of titanium as replotted from Figs. 15, 16, and 17.



(a) Untuned Specimen

RPM:
 Sweep Rate:
 Cutting Speed:
 Thickness Cut:
 Cutting Time:
 Sensitivity:

1500
 50 μ sec/cm
 2250 fpm
 .008 in.
 2.12 msec
 2 mv/cm



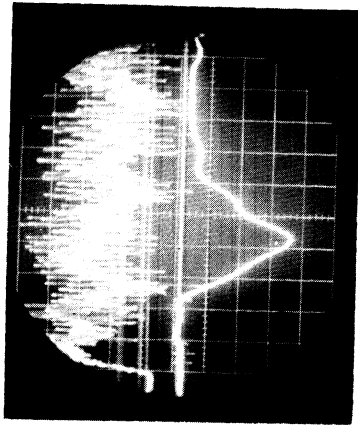
(b) Tuned Specimen

1500
 25 μ sec/cm
 2250 fpm
 .008 in.
 2.12 msec
 5 mv/cm

Fig. 21. Oscilloscope records of internal vibrations of titanium A-110 specimen. Shows the effectiveness of a tuned length of workpiece in developing large internal vibrations earlier than an untuned length. Untuned specimen was 10 in. long; tuned specimen was 3-1/4 in. long. The tuned specimen was clamped at the velocity antinodes while the untuned specimen was clamped 2 in. from the working end. Note that the strain amplitude is more than 15 times as great in the tuned specimen.

Internal
Vibrations ↑

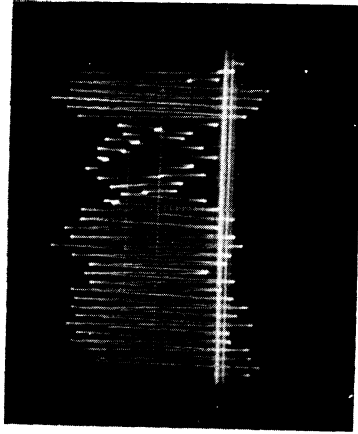
Cutting
Force ↑



(a) 1500 fpm

RPM:
Cutting Time:
Sweep Rate:
Cutting Speed:
Thickness Cut:

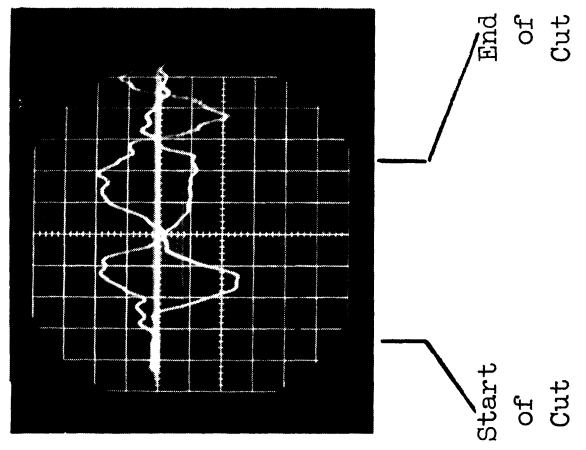
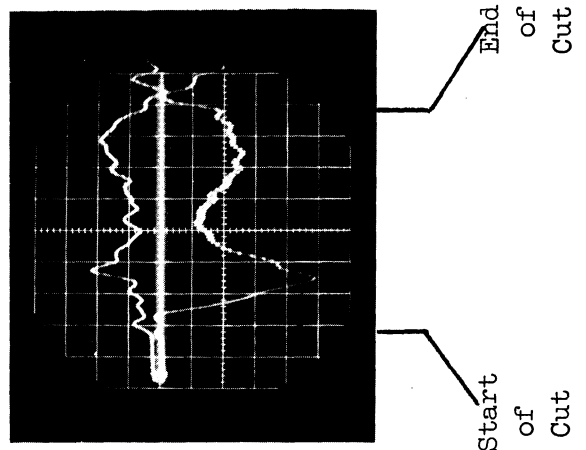
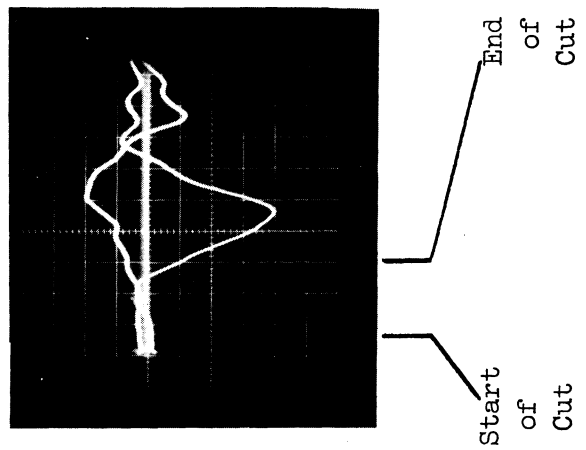
1000
3.15 msec
0.25 msec/cm
1500 fpm
.008 in.



(b) 7500 fpm

5000
0.63 msec
25 μ sec/cm
7500 fpm
.008 in.

Fig. 22. Oscilloscope records for tangential cutting force and internal vibrations of brass test specimens. Specimens were 10 in. long and were clamped 7/8-in. from working end. They developed internal vibrations early in cut because of tendency to form third harmonic. Sweep velocity was so fast that the cutting force in (b) had not had time to appear.



(a) Aluminum

(b) Brass

(c) Brass

Feeding Force ↑
Cutting Force ↓

RPM: 1250
Sweep Rate: 0.5 msec/cm
Cutting Speed: 1875 fpm
Thickness Cut: .008 in.
Cutting Time: 2.65 msec

RPM: 1000
Sweep Rate: 0.5 msec/cm
Cutting Speed: 1500 fpm
Thickness Cut: .008 in.
Cutting Time: 3.18 msec

RPM: 5000
Sweep Rate: 0.25 msec/cm
Cutting Speed: 7500 fpm
Thickness Cut: .008 in.
Cutting Time: 0.63 msec

Fig. 23. Oscilloscope records illustrating behavior characteristics of aluminum and brass test specimens. Specimens clamped 2 in. from working end inhibited development of standing waves and increased cutting forces. Note appearance of higher frequency in tangential force for brass at (b). Note also the time lag of the peak feeding force behind that for the tangential component.

APPENDIX A

TEMPERATURE MEASUREMENT

I. LEAD-SULFIDE, INFRARED DETECTOR

The basic temperature-measuring device used for most of the temperature determinations published in this Part of the Final Report was built around the lead-sulfide cell. Basically, the PbS cell is sensitive to radiation in the infrared range from about 2.1 to 2.7 microns, with sensitivity decreasing rapidly on either side of this peak region. The spectral sensitivity of the PbS cell is almost ideally suited for measurements in the temperature range of roughly 350°-1800°F. The low temperature limit is imposed on the uncooled cell by ambient thermal noise generated in the cell itself.² The upper temperature limit is imposed by the decreasing sensitivity of the cell to visible light.

A. PHYSICAL CONFIGURATION

The temperature-measuring device was enclosed in a metal tube with a layer of asbestos felt insulation to protect the housing from thermal drafts as well as from incident radiation. An aperture was located in the side of the shield so that the sensitive surface of the PbS cell could be viewed through the shield. The aperture was fitted with a nib so that a hypodermic needle could be fitted to act as a collimating device. The completed assembly was designed to be mounted below the interchangeable workpiece in such a fashion that the cutting-tool flank could be observed as it left the workpiece (see Fig. A-1).

The toolholder was a modified negative rake type which used a 1/2 in. square indexable insert. It provided a 0° end cutting edge relief angle and a -5° back rake. The insert itself was a Carboloy Grade 883 tungsten carbide insert 1/8 in. thick. The workpiece was positioned so that the cuts were made in the center of the cutting edge (see Part I of this Final Report).

B. PERFORMANCE CHARACTERISTICS

Being a semi-conductor device, the lead-sulfide cell is subject to some of the behavioral properties of semi-conductors. The most prominent effect present in the cell is the time constant due to the finite transport time involved in the motion of the holes or carriers across the semi-conductor material. The transport time is a function of the geometry of the active lead-sulfide area and hence is found to vary over considerable limits from cell to cell.

A second effect of importance is that of sensitivity—that is, the relation between the change of resistance and the change in the incident ra-

diant level. Again, this factor is a function of the specific geometry involved.

In general, it is possible to have sensitive cells with long time constants, sensitive cells with short time constants, or cells in which the two factors are "traded off." For the purposes of the work done in this report, the greatest sensitivity and the shortest response time were desirable.

Although it is not possible to measure the important geometric configuration factors directly without destroying the cell, it is possible to measure both of these attributes electrically. The relative sensitivity may be determined by measuring the change in resistance of the cell caused by exposure to a fixed level of radiation; the cell which develops the largest change in resistance is the most sensitive. The time constant may be determined by a technique similar to that used and described by Chao, Li, and Trigger.³ Fundamentally, the technique relies on the rather short ionization time of a neon lamp excited by a square-wave oscillator. A photograph of the oscilloscope trace for one of the cells tested is shown in Fig. A-2.

The time constant is defined as the time required for the cell to achieve 63.2% of its total resistance change when subjected to a step in the radiation input.

Of the several PbS cells tested, the cell selected had the highest sensitivity and nearly the shortest time constant—60 μ sec.

C. TEMPERATURE VS. OUTPUT VOLTAGE CALIBRATION

The lead sulfide cell is not an absolute device; with the introduction of the small pupil of the hypodermic needle, as well as the unknown radiant emissivity of the tungsten carbide tool insert, some form of calibration is mandatory.

Early attempts to calibrate the system involved the use of a steel rod to which the carbide tool was brazed. The steel rod was insulated and mounted in the coil of an induction heater; the comparative temperature measurement was then made with a thermocouple-potentiometer combination while the PbS cell indication was displayed on the screen of a cathode ray oscilloscope. The induction heater was used to raise the temperature of the system to around 1000°F, and then, while the system was being allowed to cool, data were collected.

The apparently sound calibration technique was subject to two rather serious sources of uncertainty or error. The temperature as measured by the PbS cell assembly was, of course, the surface temperature of the tungsten carbide tool, whereas the thermocouple measured a temperature much closer to that of the steel bar. Since data were collected while the system was in

the process of cooling, the assumption of no difference between these two temperatures was almost bound to be invalid. The second serious source of error the tarnishing effect of the high temperature. Continual and repeated exposure to temperatures of 1000°F and higher caused a considerable increase in the emissivity of the carbide surface.

These two sources of error were in opposition, yet there was no feasible manner in which their magnitudes could be evaluated; hence the dynamic technique for calibration was unacceptable. To eliminate the time-dependency of the calibration procedure a technique was devised for taking advantage of static conditions.

The influence of the tarnishing condition was eliminated by starting the temperature calibration at low temperatures. The system was calibrated by placing the tungsten carbide tool insert on an electric hot plate well shielded from drafts. As before, the thermocouple was installed in the hole in the tool insert. The system temperature was then allowed to stabilize. When the thermocouple potentiometer indicated stabilization, the fully shielded PbS cell assembly complete with hypodermic needle was brought into position over the radiant tool insert so that the initial and final trace position on the oscilloscope could be photographed.

By means of this technique, a considerable body of data was accumulated. With the exception of data for points above 800°F, the data fell well within the confidence level. The points for temperatures above 800°F were, as expected, somewhat high because of the increased surface emissivity. A log-log plot of the data indicated that a relatively simple exponential relationship could be established with precision more than adequate for test requirements. It was established that the temperature observed by the cell was

$$T = 222 (\text{mv})^{0.248}$$

where the temperature T is expressed in degrees Fahrenheit and mv is the output voltage in millivolts read from the oscilloscope trace deflection. The bridge supply voltages was maintained at 180 volts.

D. BRIDGE CIRCUITRY

The circuit used to establish the output voltage as a result of a change in cell resistance is shown in Fig. A-3. It was necessary to use a bridge arrangement primarily because the simpler voltage divider arrangement would have impressed an excessive static voltage component on the oscilloscope dc amplifiers. In essence, the two 50,000-ohm resistors and the 10,000-ohm potentiometer are a means of bucking out the static voltage so that only the voltage resulting from a change in the PbS cell resistance appears at the input of the oscilloscope. The 10-microfarad capacitor provided a low impedance path for resistor noise signals on the passive side of the bridge.

The 10,000-ohm potentiometer provided for adjustment of the balance since the resistance of the PbS cell was only nominally 1 megohm. Obviously, the leads had to be well shielded to minimize the ac hum pickup.

E. EFFECTS OF TIME CONSTANT ON RESULTS

As stated earlier, the time constant is by definition the length of time required for the cell to achieve 63.2% of its total change for a step change in input. Where the time during which the cell is exposed to radiation is in excess of the 60- μ sec time constant of the cell, the temperature as calculated from the oscilloscope trace is likely to be the closest to that actually existing at the radiant surface. However, as the exposure time becomes less than the time constant, the amount of error increases exponentially, so that if the exposure time is one half of the cell time constant, the indicated temperature is only 40% of the true temperature.

In the simplest form, the problem of evaluating the temperature traces involves a number of assumptions, some which appear to be quite valid. The static calibration procedure established the fourth power of the temperature relation, which in effect makes the instrument most sensitive to the higher temperature regions and quite insensitive to the low temperature regions. This high-value exponential relationship makes it rather safe to assume that the system actually sees a rectangular radiation pulse. But the validity of the pulse shape degenerates because of the redundancy involved in establishing the length of the pulse. In other words, the analysis has serious weakness in that the length of time during which the pulse is effective is dependent on the shape of the temperature distribution across the tool flank, and the latter is in fact the desired information.

The severity of the problem becomes apparent when one considers the length of time required for a line image to traverse the PbS cell aperture. At 1000 fpm, the time required for a line to pass the 0.0334-in.-diam end of the needle is 166 μ sec. For a line image, the observed temperature would then be 93.7% of the true value. When the width of the high-temperature area of the tool flank is greater than the line width, as most certainly it must be, the indicated value is more nearly exact. At a transit time of one-third that cited, the actual state of the tool flank is problematical, since the probable exposure time is likely to be less than the time constant of the cell.

Because of the many variables involved in the dynamic behavior of the PbS cell temperature-detection system, the observed and the actual temperature values of the tool flank become more divergent as the linear velocity of transit is increased. Such factors as the circular shape of the window, the fourth-power temperature relations, and the time constant of the cell itself make it very difficult to develop an explicit relationship between the observed and the actual temperature values. It would be highly desirable to

reduce the time constant of the detector by at least one half for the linear speeds involved, and to investigate the effects of the window shape on the system response.

Figures A-4 and A-5 show typical oscilloscope traces obtained for A-110 titanium. The blip on the left side of the trace in Fig. A-5 was caused by a titanium chip which preceded the tool flank.

F. LOCATION OF CELL RELATIVE TO WORKPIECE

Early tests run with the PbS cell and hypodermic-needle collimator were frequently inconsistent, wide variations in indicated temperature being observed for identical test conditions. The eye of the needle was initially placed so that it would observe the tool flank immediately after it had left the work. It was found that in many cases the trailing edge of the material was being turned over and was in effect blocking the view of the system.

A series of tests were run in an effort to establish the effect of spacing the needle away from the trailing edge of the work. It was observed that the amplitude of the measurement increased in a somewhat erratic manner until the needle was spaced out about 0.075 in. The indications remained relatively constant until the needle was spaced 0.120 in. from the work, at which distance they decreased detectably. Since the turned edge normally extended out 0.040 in., the needle space was set at 0.090 in., which was considerably more than minimum and enough less than maximum so that suitable results might be expected.

G. OSCILLOSCOPE TRIGGERING

1. Technique

The Tektronics type 502 oscilloscope is equipped with a single-sweep circuit so that it may be armed and fired once for a single trace if desired. The lower trace circuitry of the oscilloscope was used with a signal from a magnetic pickup located on the lathe spindle to establish the trigger point for the single sweep. The position of the sweep relative to the tool-work position was adjusted by moving the magnetic pickup position on the lathe spindle. Through the use of the technique described, it was possible to display the complete temperature trace for any selected chip.

2. Procedure

In most cases, the test procedure required a total feed to five chip thicknesses. This depth of feed was established by the proper setting of

the feed rate and the feed-stop micrometer. While the feed-stop-micrometer adjustment was being made, the oscilloscope-sweep-arming-micrometer adjustment was also made so that the fourth or next to last chip would be recorded.

The likelihood that the tool and workpiece would engage so as to produce a first chip of full thickness was remote, as was the likelihood that, the last chip would be complete or of full thickness. There was no reason to suspect that the thickness of the middle three chips would be other than that desired; therefore the triggering of the sweep was planned for the next to the last sweep. All the records thus made were for this fourth last chip.

II. THERMOCOUPLE IMBEDDED IN TOOL

For comparative purposes a series of tests were run with a thermocouple imbedded in the carbide tool insert. The insert was provided with a hole so proportioned that the thermocouple was located approximately 0.020 in. from the leading edge of the tool. The output of the thermocouple was used to drive a low-level Sanborn amplifier and recorder. Since the time constant of the tool-thermocouple system was of the order of 3 or 4 sec, the limited frequency response of the Sanborn system was more than adequate. Aside from the absence of a triggering requirement, the procedure used was the same as that used for the PbS test runs. Figure A-6 shows the tool-thermocouple assembly mounted in the lathe.

The toolholder used for these tests was a Kennametal KSFR-85A negative rake type that was shifted to provide a 0° end cutting edge angle. It also created a -5° back rake. The inserts used were Carboloy Grade 883, of $1/2$ in. square size, with the thermocouple imbedded in the middle of the active cutting edge.

APPENDIX B

STRAIN-GAGE INSTRUMENTATION

In order to monitor the longitudinal vibrations of the workpiece, strain gages were applied to the periphery of the bar. To obtain the maximum possible strain sensitivity, along with other advantages, a ballast circuit was used (see Fig. B-1).

Theoretically, the ballast circuit used with the gages positioned as shown in Fig. B-2 will not respond to bending loads. For the circuit output to be independent of bending, the states of strain due to bending in both gages must be equal in magnitude and opposite in sign. More accurately, it should be stated that the resistance changes in the gages due to a bending moment should be equal but of opposite sign.

To meet the conditions of the exact theory, each gage must be the same distance from the neutral axis and the gage factors of the gages must be exactly the same. As these conditions are practically impossible to obtain, however, a suitable compromise must be made on the basis of expected magnitudes and planes of action of bending moments.

By trying to place the gages on the neutral axis related to the maximum expected bending moment, minimum output due to this component of bending can be achieved. From Fig. B-2 it can be seen that the effect of bending due to the cutting force was minimized by using this method.

As negligible radial force is to be expected, the theoretical cancelling effect of the circuit enables one to predict that any output caused by this force should be extremely small compared with the longitudinal vibration output. Therefore it can be neglected.

The output from the ballast circuit can be expressed as:

$$e_o = (KRI)\epsilon$$

where: e_o is output voltage
 ϵ is unit strain
K is the gage factor
R is the gage resistance
I is the circuit current

It can be expected that the battery voltage will drop slightly during the test, leading to slightly low output voltages. The ballast resistor used was a 15,000-ohm, 1-watt resistor, and the voltage source was a 300-v instrument battery.

Table B-I contains all the pertinent information on the strain gages. The gages were mounted by means of Fix-Mix epoxy resin cured 24 hours at 70°F with a post-cure of 1 hour at 120°F.

TABLE B-1

SEMI-CONDUCTOR STRAIN-GAGE DATA

| Test Specimen | Resistance* (ohm) | Gage Factor** | Mfg. Type No. |
|----------------|----------------------|---------------|---------------|
| Brass | 356 | 119 | MS 302 - 350 |
| Aluminum | 356 | 119 | MS 302 - 350 |
| A-110 Titanium | 347 | 103 | NA3-16 - 350 |
| 1018 Steel | 355 | 122 | MS 302 - 350 |
| Copper | 347 | 103 | NA3-16 - 350 |
| Magnesium | 355 | 95 | NA3-16 - 350 |

*Tolerances on resistances are 1%.

**Tolerances on gage factors are 2%.

A test run made to determine if the semi-conductor strain gages generated any spurious signals gave a satisfactory negative result. The test was made using the highest possible oscilloscope sensitivity (200 $\mu\text{v}/\text{cm}$) and showed a slight but generally negligible spurious output. For this test, the battery was removed from the circuit and the 15,000-ohm resistor shorted across the strain-gage output loads. The voltage of the supply battery was constantly checked so that the actual circuit characteristics could be accurately predicted.

To check the actual output of the circuit related to a known resistance change in the gages, a 230,000-ohm resistor was chopped in and out of the circuit across the gages. This produced a resistance change equivalent to that which would have been caused by a 25- $\mu\text{in.}/\text{in.}$ strain in the gages. The resulting oscilloscope response was exactly the same as that predicted by the theory.

APPENDIX C

CUTTING-FORCE MEASUREMENTS

A special clamp was constructed so that the cylindrical workpieces could be supported by the measuring element of a three-force dynamometer. It was hoped that in this manner the feeding and cutting components of force could be measured (see Fig. C-1).

The dynamometer was fitted with highly rigid load cells. The natural frequency of vibration in both the cutting and feeding direction was found to be approximately 5000 cps. A check of the free vibration of the dynamometer indicated that the damping factor (c/cc) was only about 0.02.

In general, from knowledge of the free-vibration characteristics of the dynamometer it can be said that for force fluctuations whose effective frequency is less than 7000 cps, the dynamometer will indicate a high value of force; that for frequencies less than 1000 cps the dynamometer output will be less than 5% too high; and that for frequencies greater than 7000 cps the output will be greatly attenuated.

Due to the attenuation of high-frequency vibratory force components, it was expected that the chip-segmentation frequencies, which had occurred at between 50,000-250,000 cps on previous tests, could not be observed on the dynamometer force records. However, the mean component of cutting force should easily be observed.

Due to the low damping present, all force traces were expected to exhibit some degree of overshoot due to the initial contact of the tool and the workpiece. For the slower cutting rates (1500 fpm) the force traces exhibited this overshoot, but quickly settled down to steady values. For the fastest cutting rates (7500 fpm) sufficient time was not available to allow the dynamometer to recover from the overshoot and attain a steady value during the cut.

APPENDIX D

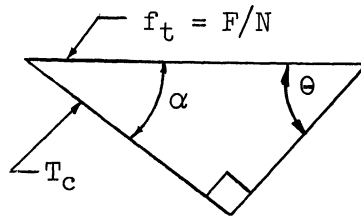
WEAR STUDIES

SINGLE-TOOTH CUTTER

The initial studies of single-point cutting-tool wear were carried out using a Wesson 1-1/4-in.-diam EM-100-40 2-tooth milling cutter accurately mounted in the Alcoa high-speed lathe. Only one insert acted as a cutting edge, the opposite insert being relieved to avoid cutting the workpiece. Figure D-1 shows the cutter installed. Inserts used were Wesson ABC-2442 Grade 61 style.

Wear studies were made by feeding a workpiece perpendicularly to the axis of rotation of the cutter at a measured and controlled feed rate. The workpiece, of A-110 titanium, was 0.100 in. wide and 12 in. long. A cleanup cut was made prior to each series of tests so that each new portion of the cutting edge used was exposed to the same initial cutting conditions. A particular series consisted of eight cutting passes across the workpiece. Observations of cutting action were made during each series of runs, the depth of cut was adjusted for the same depth between individual passes, and surface finish was observed and measured after eight passes. The wear of the cutting edge, both flank and top face was then observed and measured, with appropriate sketches being included in the summary data sheet. Since the actual cutting edge was about 1 in long, several series could be run along a single edge, providing a direct comparison of flank and face wear under different cutting conditions.

The parameters of interest related to tool wear were cutting velocity, tool-workpiece contact time, feed rate of the workpiece, depth of cut, and maximum thickness of the chip. Previous experience dictated that the contact time between the tool and the workpiece be limited to a maximum of 1 msec, with shorter times, down to 333 μ sec, more desirable. A fixed depth of cut of 0.015 in. was established so that the chip thickness would be related to the feed rate as indicated in Fig. D-2.



$$\sin \alpha = \cos \theta = (R-d)/R \quad (1)$$

$$\text{For } d = 0.015 \text{ in.}; \quad \alpha = 77^\circ 25' \quad (2)$$

$$F_t = f \times N \quad (3)$$

$$F = f_t \times N \quad (3)$$

$$T_c = f_t \cos \alpha$$

$$T_c = F/N \cos \alpha \quad (4)$$

For $d = 0.015 \text{ in.}; \quad \cos \alpha = 0.21786$

$$\therefore T_c = .21786 f_t \quad (5)$$

$$= .21786 F/N \quad (6)$$

$$t_c = \frac{\frac{\theta}{360}}{\frac{N}{60}} = \frac{\theta}{360} \times \frac{60}{N} = \frac{\theta}{6N} \quad (7)$$

For $d = 0.015 \text{ in.}; \quad \theta = 12''35'$

$$\therefore t_c = \frac{12.5833}{6N} \text{ sec} \quad (8)$$

$$\therefore t_c = \frac{12583333}{6N} \mu\text{sec} \quad (9)$$

Conditions selected were such that a feed rate of 0.0367 ipt with a 0.015-in. depth of cut would yield an 0.008-in.-thick chip with cutter speeds varying to limit contact times from 1000 μsec to 333 μsec with table feeds from 38.6 up to 154 ipm. The contact times covered the range which had been found in previous work to be most favorable. The workpiece was fed into the cutter so that climb milling took place.

Table D-I is a typical data sheet of the results of those different single-tooth wear tests based on eight passes.

II. MULTITOOTH CUTTERS

The single-tooth wear studies pointed the direction for increased metal removal rates through the rise of multiple-tooth, small-diameter cutters driven at high speeds.

These evaluation tests were made by mounting a small 2-hp high-speed air turbine in place of the tool holder on the cross-rail of a 36-in. hydraulic planer. National Twist Drill No. 567 solid tungsten carbides 4-fluted spiral milling cutters of 1/4-, 5/16-, 3/8-, and 1/2-in. diameters were mounted in

the chuck of the turbine, which was driven at the maximum speed possible with the existing air supply. Suitable workpieces with a section 0.100-in. and 12 in. long were mounted on the planer table. Cutting was initiated by feeding the workpiece into the rotating cutter to provide climb milling feed. Several passes of the workpiece by the cutter, with fixed depths of cut being taken every pass, constituted cutting action. Figures D-3 and D-4 show the relative positions of the cutter and workpiece. A series of five passes was made across the workpiece with the depth of cut being adjusted after each pass. At the end of five passes, the cutter was removed and the flank wear of each of the four cutting edges was measured at the cutting area. Cutting was continued until failure occurred.

The cutter was then raised or lowered to provide new unused cutting edges along the length of the cutter, so that tool wear under several different conditions could be measured and compared. The turbine would slow down approximately 2000 rpm during each pass, but would return to its maximum speed of 19,400 rpm during the return stroke of the workpiece.

With cutters of the size used, the cutting velocities varied from about 1200 fpm for a 1/4-in. cutter to about 2500 fpm for a 1/2-in. cutter. The same geometric relations as shown in Fig. A-2 prevail for this mode of cutting, so that with a depth of cut of 0.015 in., cutting edge-workpiece contact time were in the range of 175 to 275 μ sec when the table feed rates varied from 20 to 100 fpm. This provided feed rates of 0.003 to 0.017 ipt for 4-tooth cutters, which resulted in chip thickness from 0.001 to 0.014 in. Cutters were individually selected for minimum runout between the lands and were oriented for minimum runout when installed in the turbine.

Table D-II shows the relationship that existed in these high-speed milling tests. Tables D-III and D-IV are typical data sheets.

III. OBSERVATIONS ON CUTTER WEAR

On the basis of these wear studies, the following observations can be made:

1. The flank wear is commonly most serious at the trailing portion of the cutter zone (see Figs. D-5 and D-6).
2. The most severe burr upon the edge of the workpiece accompanied the area of greatest wear of the cutting edges.
3. The flank areas directly behind wear zones are commonly covered with spots of fused material, giving a blistered effect.

4. Heavy wear trends are common to one side of the cutters.
5. Chip weld to tools is common to all cuts.
6. Surface finish is that left by the one tooth making deepest cut.

TABLE D-I

TYPICAL DATA SHEET

(Three Different Single-Tooth Wear Tests)

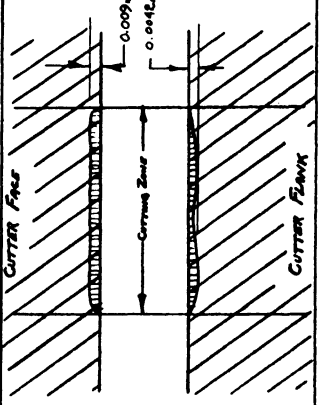
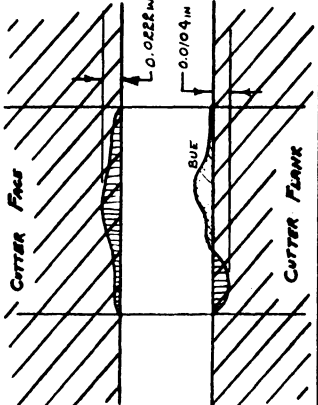
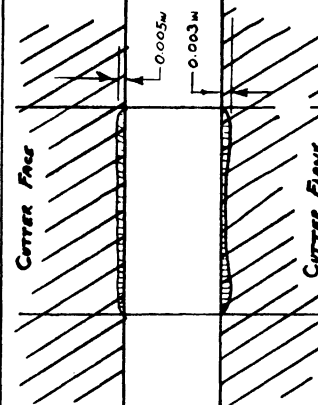
| MATERIAL - TITANIUM A-110 | | DATA REDUCTION SHEET | | | | | | | ALCOA HIGH-SPEED LATHE MICROMILLING SINGLE-TOOTH CUTTER | | |
|---------------------------|---------------------|----------------------|--------------------|-------------------------------|----------------------|------------------|-------------------------|---------------|--|---|---|
| RUN # DATE | SPINDLE SPEED (RPM) | CUTTING SPEED (FPM) | DEPTH OF CUT (IN.) | CUTTING TIME PER TOOTH (MIN.) | FEED PER TOOTH (IPR) | TABLE FEED (IPM) | RMS SURFACE FINISH (RA) | NO. OF PASSES | TOOL NO. | TYPE OF CUTTING ACTION | MICROSCOPIC CUTTER ANALYSIS |
| A-8 11-6-62 | 2100 | 687.2 | 0.015 | 1000 | 0.0367 | 77 | 30-40 | 8 | B-1 | clean cutting action no sparks or welded chips throughout entire eight passes. no burr noted. |  |
| B-8 11-7-62 | 4200 | 1374.24 | 0.015 | 500 | 0.0367 | 154 | 85-115 | 8 | B-2 | continuous white spark noted at approximately the fifth pass and continued through eighth pass. quality of cutting action steadily decreased burr noted after sixth pass. |  |
| C-8 11-8-62 | 4200 | 1374.24 | 0.015 | 500 | 0.0183 | 77 | 40-60 | 8 | B-3 | clean cutting action thru first three passes. After fourth pass sparking occurred thru seventh pass becoming continuous spark on eighth pass. burr continued after third pass. |  |

TABLE D-II

RELATION OF VARIOUS PARAMETERS FOR MULTITOOTH-CUTTER WEAR STUDIES
 (0.015-in. depth of cut, 19,400-rpm cutter speed)

| Cutter Diameter, in. | Cutting Velocity fpm | Tool Contact Time, μ sec | Table Speed, fpm | Table Feed, ipt | Chip Thickness, in. |
|----------------------------|----------------------------|------------------------------------|------------------------|-----------------------|---------------------------|
| 1/4 | 1270 | 244 | 20 | .0034 | .0016 |
| | | | 40 | .0069 | .0033 |
| | | | 60 | .0103 | .0048 |
| | | | 83.3 | .0143 | .0068 |
| | | | 100 | .0172 | .0082 |
| 5/16 | 1590 | 217 | 20 | .0034 | .0013 |
| | | | 40 | .0069 | .0029 |
| | | | 60 | .0103 | .0044 |
| | | | 83.3 | .0143 | .0061 |
| | | | 1000 | .0172 | .0073 |
| 3/8 | 1900 | 198 | 20 | .0034 | .0013 |
| | | | 40 | .0069 | .0027 |
| | | | 60 | .0103 | .0040 |
| | | | 83.3 | .0143 | .0056 |
| | | | 100 | .0172 | .0068 |
| 1/2 | 2561 | 172 | 20 | .0034 | .0012 |
| | | | 40 | .0069 | .0023 |
| | | | 60 | .0103 | .0035 |
| | | | 83.3 | .0143 | .0049 |
| | | | 100 | .0172 | .0059 |

TABLE D-III

TYPICAL DATA SHEET

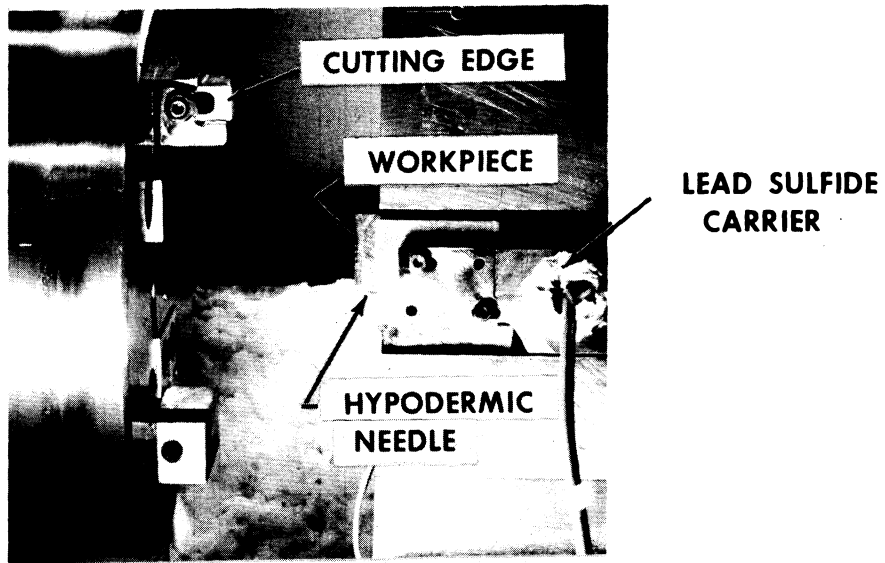
(Test Runs Nos. 1, 2, and 3)

CARBIDE MILL PROGRAM PNEUMATIC AIR TURBINE MILL
 J. E. RAMSEY, JR. ROCKFORD PLANT

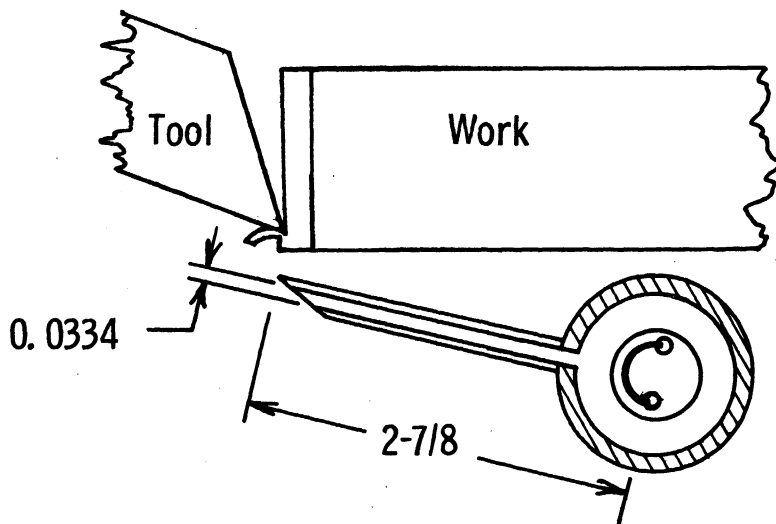
| MATERIAL | EC. - A-110 | No. of Passes 10 | | SURFACE FINISH | OBSERVATIONS | AV. WEAR | TOOTH FLANK INSPECTION |
|---------------------------------|-------------|------------------|-----|---|--|---------------------|------------------------|
| TEST RUN # 1 | 11-27-62 | 1/4 | IN | | | | |
| CUTTER DIA. | 1/4 | 4 | | | | 0.0170" 2 205 | |
| No. of TEETH | 4 | | | | | 0.0176" 3 250 | |
| CUTTING SPEED | 1270 RPM | 60 | FPM | | | 0.0064" 4 33 | |
| TABLE SPEED | 60 | | | | | | |
| DEPTH of CUT | 0.015 | | IN | | | | |
| CUTTER ZONE CODE 1/4 - 1 - B | | | | | | | |
| TEST SERIES # 2 | 11-27-62 | 1/4 | IN | BAD CHIPS WELDED ON BURR BASIC SURFACE HAS IMPROVED OVER SERIES 1 | red hot cut observed turbine held speed chips irregular shaped & distorted | 0.0028" 1 35 | |
| CUTTER DIA. | 1/4 | 4 | | | | 0.0052" 2 35 | |
| No. of TEETH | 4 | | | | | 0.0085" 3 40 | |
| CUTTING SPEED | 1270 RPM | 40 | FPM | | | 0.0020" 4 35 | |
| TABLE SPEED | 40 | | | | | | |
| DEPTH of CUT | 0.015 | | IN | | | | |
| CUTTER ZONE CODE 1/4 - 1 - C | | | | | | | |
| TEST SERIES # 3 | 11-27-62 | 1/4 | IN | NICE SMALL BURR CLEAR SURFACE | orange cut turbine slowed slightly | 0.0028" 1 35 | |
| CUTTER DIA. | 1/4 | 4 | | | | 0.0045" 2 35 | |
| No. of TEETH | 4 | | | | | 0.017" 3 35 | |
| CUTTING SPEED | 1270 RPM | 20 | FPM | | | 0.0015" 4 35 | |
| TABLE SPEED | 20 | | | | | | |
| DEPTH of CUT | 0.015 | | IN | | | | |
| CUTTER ZONE CODE 1/4 - 1 - D | | | | | | | |

REFERENCES

1. Colwell and Quackenbush, "A Study of High-Speed Milling of Titanium Alloys," ORA Report 04393-8-F, The University of Michigan, Ann Arbor, December, 1961.
2. Klassen and Blok, Physica, Vol. XXIV, pp. 975-984, December, 1958.
3. Chao, Li, and Trigger, "Experimental Determination of Temperature Distribution at Tool Flank and Evaluation of Frictional Energy Distribution Over Tool-Chip Contact," ORD-1980-5, University of Illinois.



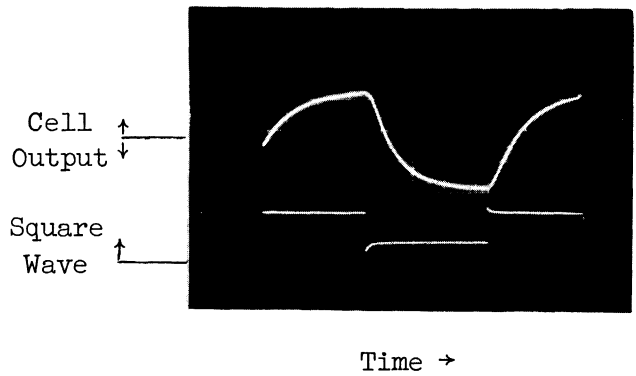
(a) Lead-sulfide cell and workpiece mounted in lathe.



Lead Sulfide Cell
and Needle Collimator

(b) Schematic section of details.

Fig. A-1. Temperature-measuring set-up used to obtain data plotted in Figs. 13-20.



Time Constant Test

Fig. A-2. Oscilloscope trace for one of lead-sulfide cells tested. Time constant of cell was determined from output created by neon tube driven by a square-wave oscillator. Sweep velocity was 5 $\mu\text{sec}/\text{cm}$; frequency was 5 kc.

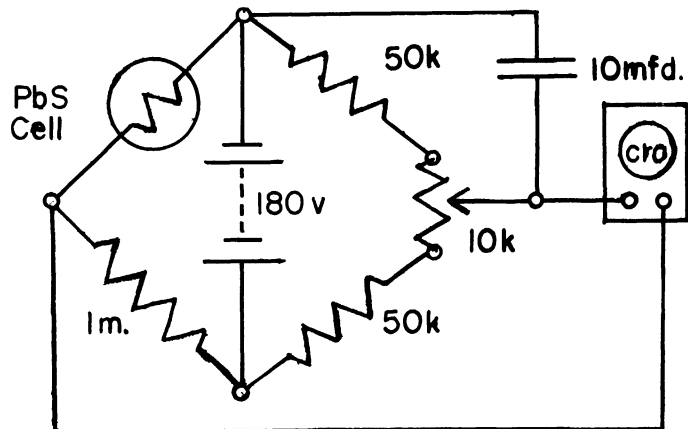
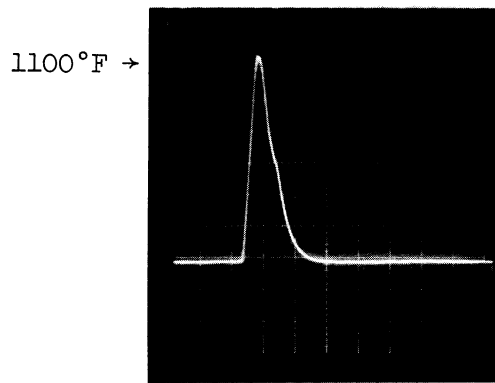


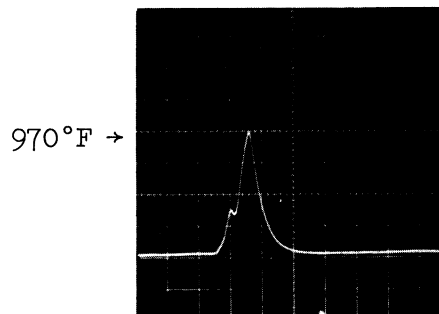
Fig. A-3. Bridge circuit used with lead-sulfide cell for temperature measurement.



Time →

A-110-3

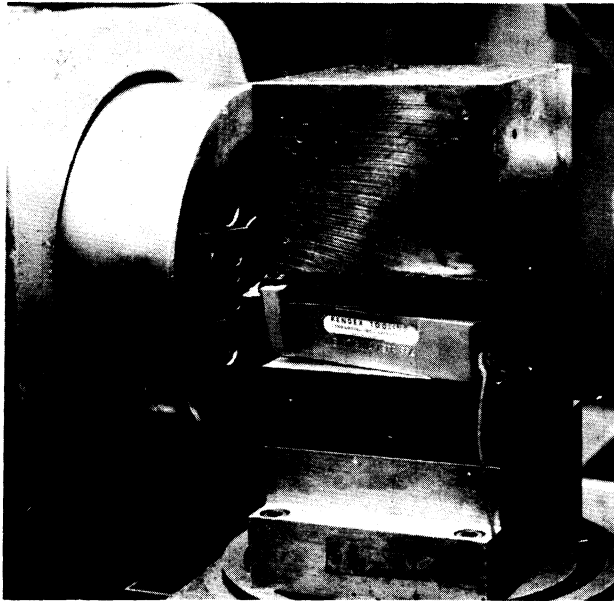
Fig. A-4. Oscilloscope trace of tool-flank temperature (A-110 titanium, 1-in. cut). Titanium cut at feed of 0.002 ipt. Flank of tool insert required 316 μ sec to pass by hole in the hypodermic needle. Sweep velocity: 500 μ sec/cm. Cutting speed: 2500 fpm. Sensitivity: 100 mv/cm.



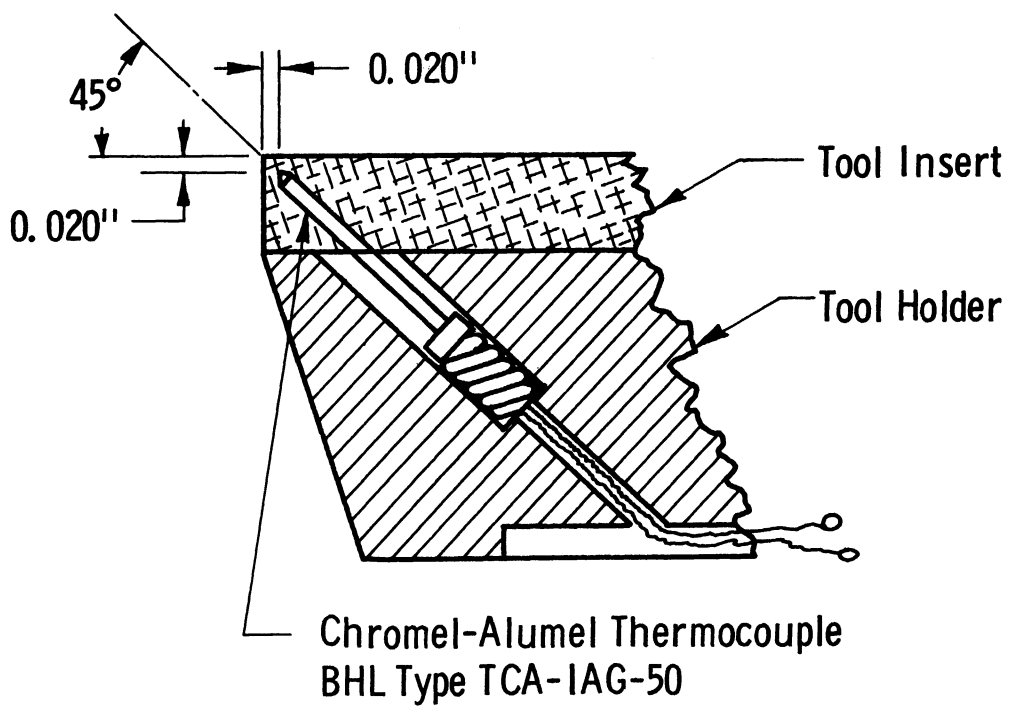
Time →

A-110-13

Fig. A-5. Oscilloscope trace of tool-flank temperature (A-110 titanium, 1/2-in. cut). Test conditions and oscilloscope settings same as for Fig. A-4 except for length of cut. Blip on left side of trace caused by titanium chip which clung to cutting tool.



(a) Thermocouple-tool assembly mounted in lathe.



(b) Schematic section showing location of thermocouple.

Fig. A-6. Temperature-measuring set-up used to obtain data plotted in Figs. 6-12.

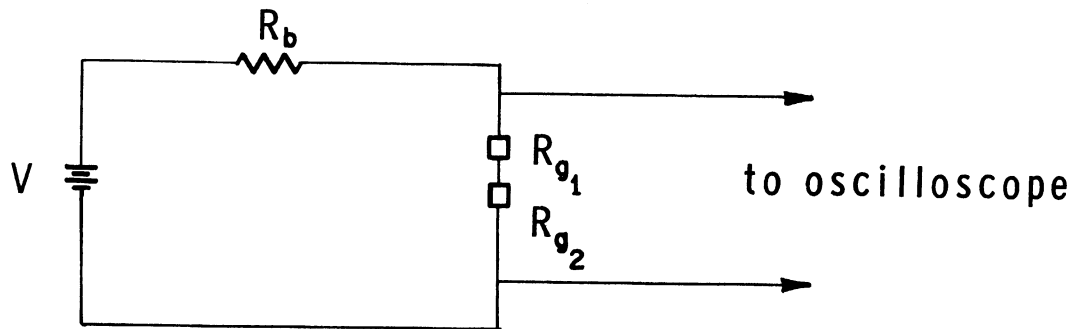


Fig. B-1. Ballast circuit used with strain gages.

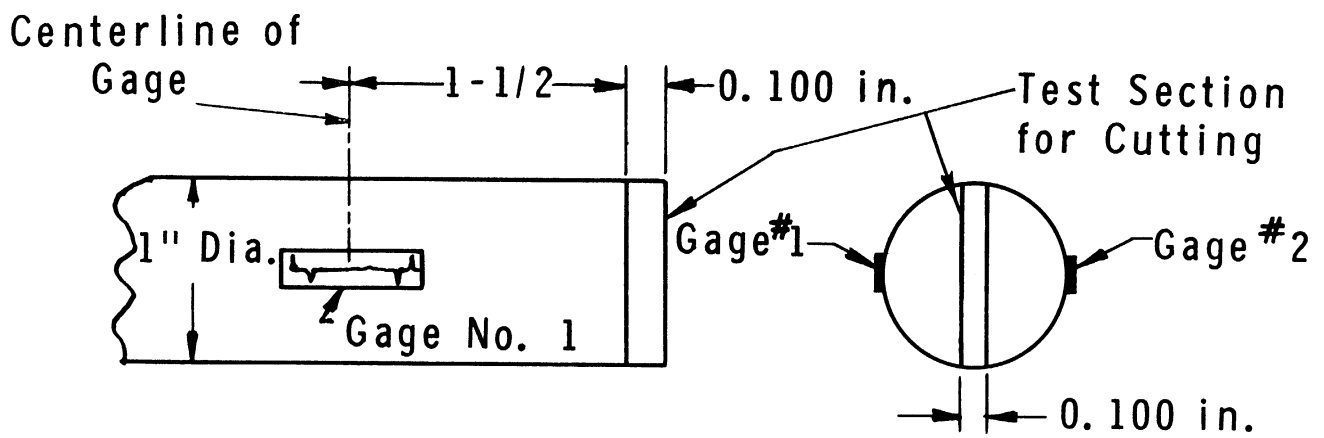


Fig. B-2. Location of strain gages used to monitor internal vibrations as displayed in Figs. 21 and 22.

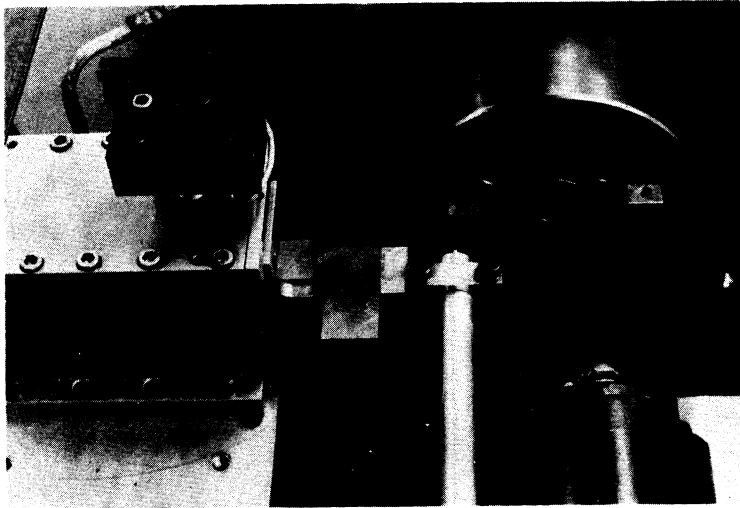


Fig. C-1. Set-up used to obtain cutting-force records shown in Figs. 22 and 23. Output of dynamometer shown at left was displayed on a Tektronix 502 oscilloscope. Workpiece is 1-in.-diam rod at lower center.

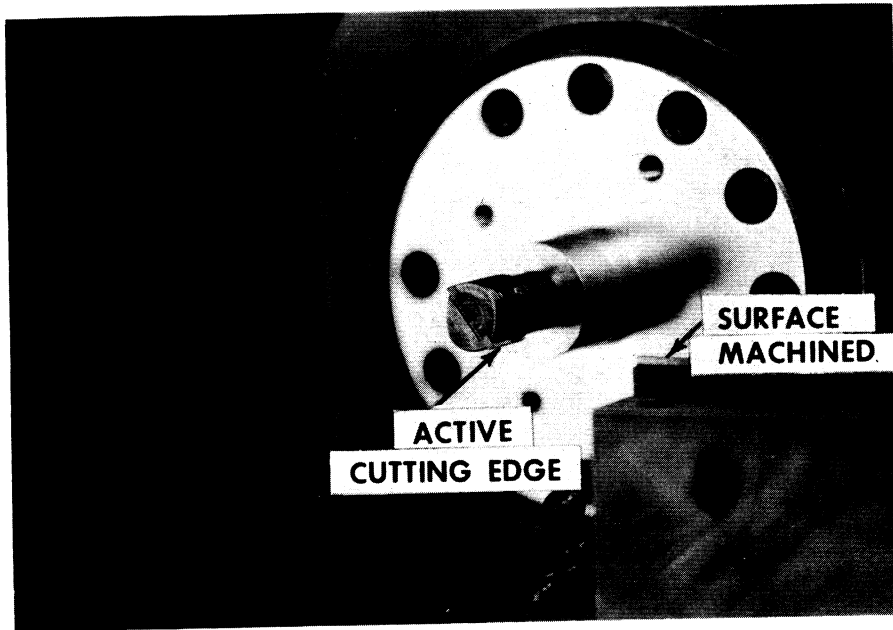


Fig. D-1. Set-up for studies of single-tooth-cutter wear. Cutter 1-1/2 in. in diameter with tungsten carbide insert. Cutter mounted in spindle of Alcoa lathe. Workpiece A-110 titanium alloy.

F = Workpiece Feed Rate, Inches/Min.
 f_t = Cutter Feed Per Tooth, in.
 t_c = Contact Time, Seconds
 T_c = Max. Chip Thickness in.
N = Cutter Revolutions Per Min.

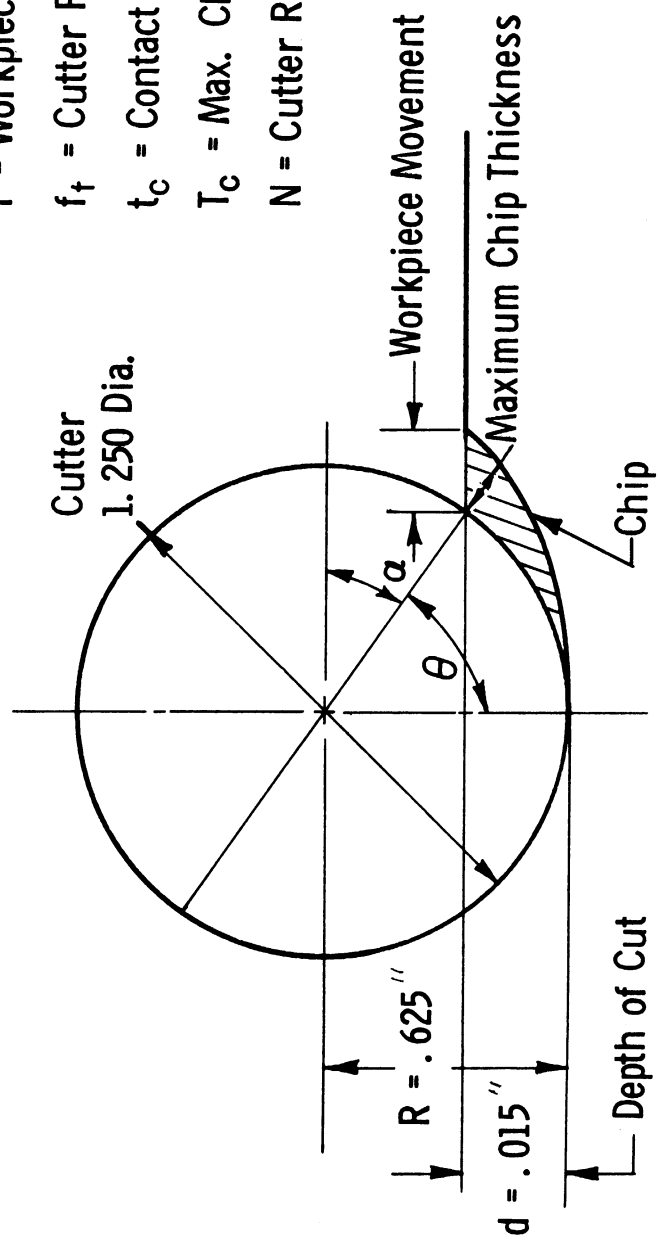


Fig. D-2. Relation between chip thickness and feed rate.

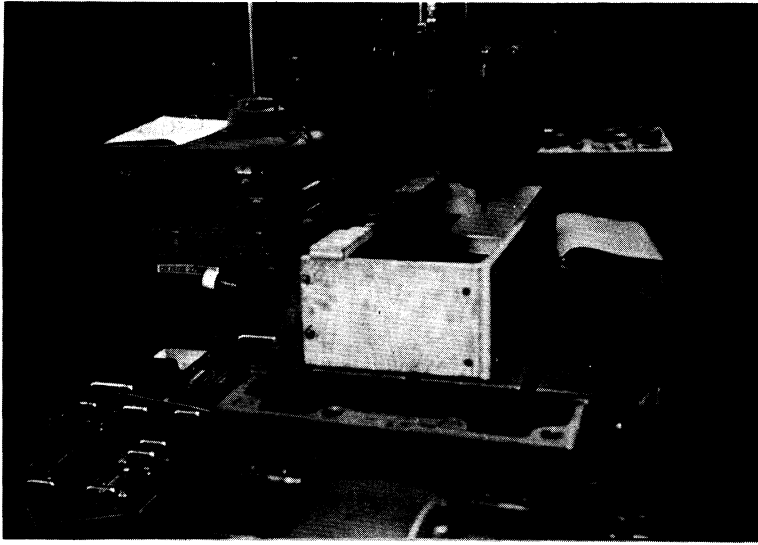


Fig. D-3. End view of partially enclosed set-up showing instrumentation.

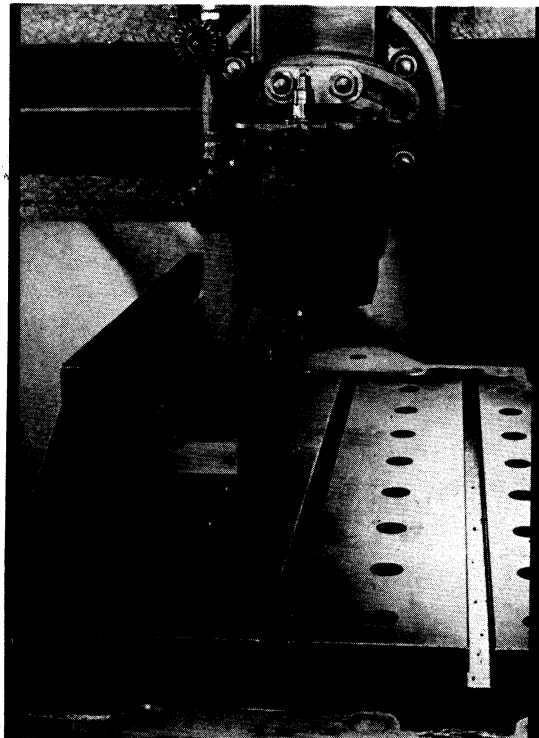


Fig. D-4. Open end view of cutter and workpiece orientation.

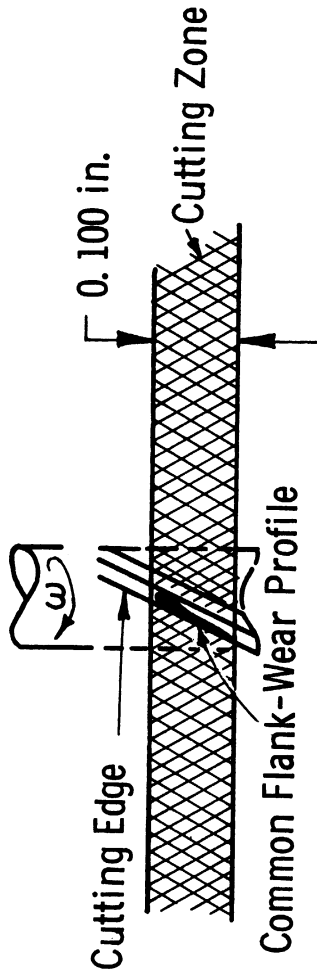


Fig. D-5. Common flank-wear profile.

TOOTH FLANK INSPECTION

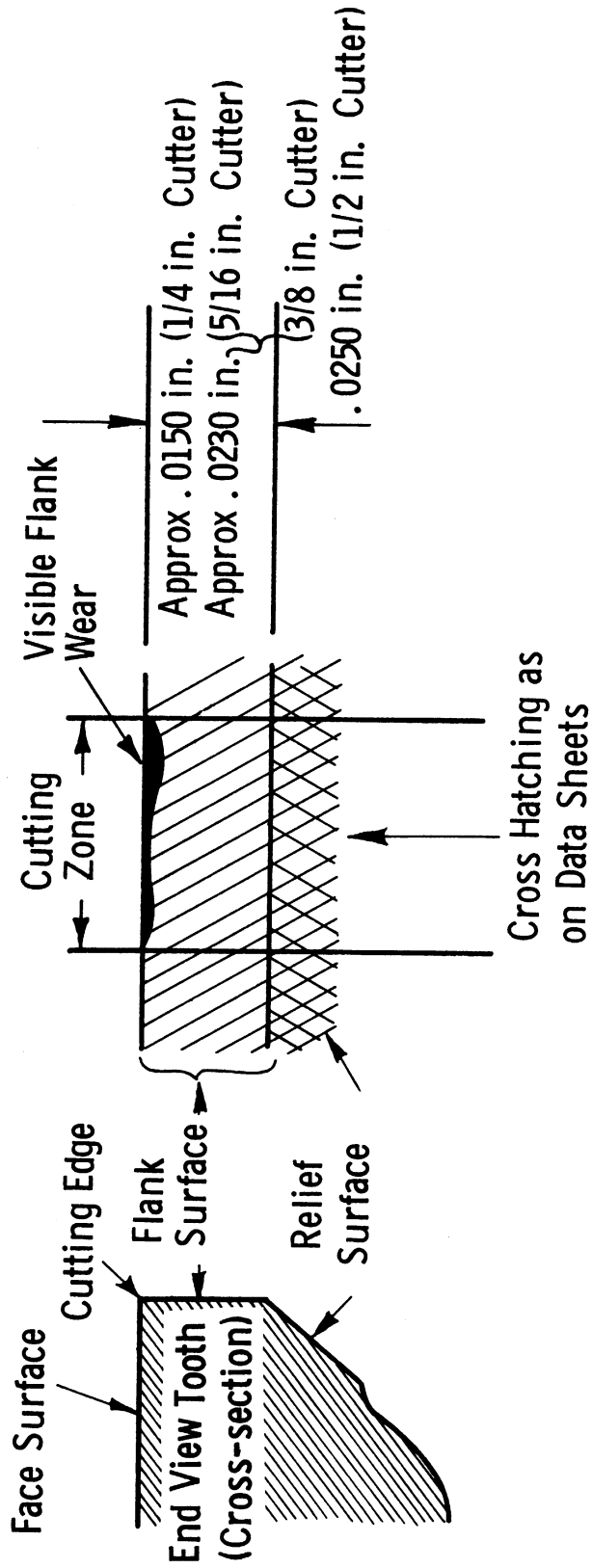


Fig. D-6. Sketch of typical wear of 4-fluted tungsten carbide milling cutter.

UNIVERSITY OF MICHIGAN



3 9015 02841 2362